

# CDMFT+HFD : an extension of dynamical mean field theory for nonlocal interactions applied to the single band extended Hubbard model

S. Kundu<sup>1\*</sup> and D. Sénéchal<sup>2</sup>

<sup>1</sup> Department of Physics, University of Florida, Gainesville, FL 32611, USA

<sup>2</sup> Département de physique and Institut quantique, Université de Sherbrooke, Sherbrooke, Québec, Canada J1K 2R1

\* [sarbajay.kundu@ufl.edu](mailto:sarbajay.kundu@ufl.edu)

## Abstract

We examine the phase diagram of the extended Hubbard model on a square lattice, for both attractive and repulsive nearest-neighbor interactions, using CDMFT+HFD, a combination of Cluster Dynamical Mean Field theory (CDMFT) and a Hartree-Fock mean-field decoupling of the inter-cluster extended interaction. For attractive non-local interactions, this model exhibits a region of phase separation near half-filling, in the vicinity of which we find pockets of  $d$ -wave superconductivity, decaying rapidly as a function of doping, with disconnected patches of extended  $s$ -wave order at smaller (higher) electron densities. On the other hand, when the extended interaction is repulsive, a Mott insulating state at half-filling is destabilized by hole doping, in the strong-coupling limit, in favor of  $d$ -wave superconductivity. At the particle-hole invariant chemical potential, we find a first-order phase transition from antiferromagnetism (AF) to  $d$ -wave superconductivity as a function of the attractive nearest-neighbor interaction, along with a deviation of the density from the half-filled limit. A repulsive extended interaction instead favors charge-density wave (CDW) order at half-filling.

Copyright attribution to authors.

This work is a submission to SciPost Physics Core.

License information to appear upon publication.

Publication information to appear upon publication.

Received Date

Accepted Date

Published Date

1

## 2 Contents

3	<b>1 Introduction</b>	2
4	<b>2 Model and method</b>	4
5	2.1 Model Hamiltonian	4
6	2.2 Method: CDMFT+HFD	4
7	<b>3 Results</b>	7
8	3.1 Phase diagram at the particle-hole symmetric chemical potential	7
9	3.1.1 $V < 0$ :	7
10	3.1.2 $V > 0$ :	12
11	3.2 Phase diagram as a function of density	12
12	3.2.1 $V < 0$ :	12
13	3.2.2 $V > 0$ :	16

14	<b>4 Discussion and conclusions</b>	<b>17</b>
15	<b>A Appendix</b>	<b>20</b>
16	<b>References</b>	<b>22</b>

---

## 19 **1 Introduction**

20 The single-band Hubbard model has long served as a useful platform for studying the effect of  
21 strong electronic correlations [1–6]. In particular, it explains many of the experimental obser-  
22 vations in the high- $T_c$  cuprate superconductors [2, 7–16], providing an approximate picture for  
23 the description of these materials [17–25]. More recently, there have been numerous studies  
24 on extensions of this model with nearest-neighbor interactions, known as the extended Hub-  
25 bard model (EHM) [26–90]. There are several reasons for the continuing interest of the com-  
26 munity in exploring the effect of non-local interactions. In actual materials, the interactions  
27 between neighboring sites may not be completely screened, necessitating a more careful treat-  
28 ment of longer-range interactions. The model with an attractive nearest-neighbor interaction  
29 provides an effective representation of the attractive interactions mediated by electron-phonon  
30 coupling, and may be realized in ultra-cold atom systems. The relevance of studying such a  
31 model is further emphasized by recent ARPES studies on the one-dimensional cuprate chain  
32 compound  $\text{Ba}_{2-x}\text{Sr}_x\text{CuO}_{3+\delta}$  [91], where the observations can be explained using a Hubbard  
33 model with an attractive extended interaction. On the other hand, the model with repulsive  
34 non-local interactions provides an ideal playground for studying the interplay of charge and  
35 spin fluctuations, since the relative magnitude of the charge fluctuations can be controlled by  
36 the strength of the extended interaction [26, 30, 34, 35]. The EHM at quarter-filling has proven  
37 useful for describing the charge ordering transition due to inter-site Coulomb interactions in  
38 a variety of materials [28, 48, 49, 79, 83]. Both the Hubbard model and its extension with  
39 longer-range interactions have contributed significantly to the methodological development  
40 in the field of strongly correlated systems, and in particular high- $T_c$  superconductors, which is  
41 essential for obtaining results that can be quantitatively compared with experiments.

42 In recent years, the properties of the EHM have been analyzed using a variety of ap-  
43 proaches, including, among others, mean-field theory [50–52, 72], functional renormalization  
44 group (fRG) [39], exact diagonalization (ED) [29, 32, 55, 61], density-matrix renormalization  
45 group (DMRG) [57, 63], Quantum Monte Carlo (QMC) [70, 87, 89, 92] and the fluctuation-  
46 exchange approximation (FLEX) [56]. However, many of the approaches used are best suited  
47 for studying the weak-coupling or the strong-coupling limit, and there are few that can de-  
48 scribe the intermediate-coupling regime equally well. Even among those that can, each has its  
49 own limitations. For instance, simple exact diagonalizations are restricted to small systems,  
50 quantum Monte Carlo methods suffer from the fermion sign problem in many applications  
51 of interest, the density-matrix renormalization group (DMRG) applies to one-dimensional or  
52 ribbon-like systems, etc. In addition, certain aspects of the model with repulsive interactions  
53 have been studied in detail using the so-called extended dynamical mean-field theory (EDMFT)  
54 approach [93–95], in which the local density fluctuations together with the local self-energy  
55 are propagated on the whole lattice using the known dispersion and density-density extended  
56 interactions. Other variations of this method, such as a combination of EDMFT with the GW  
57 approximation [27, 96–98], which perturbatively includes non-local self-energy corrections,  
58 and the dual boson method [81, 82, 99], which constructs a diagrammatic expansion about

59 the extended DMFT, have likewise contributed to its understanding. More recently, cluster  
 60 methods [26, 38, 76–78, 100, 101], which capture short-range correlations non-perturbatively  
 61 within periodic clusters, have also been applied to this model. However, such studies have  
 62 largely been limited to fixed densities and repulsive interactions. Overall, there have been  
 63 fewer studies that consider both an extensive range of interaction couplings and band fillings,  
 64 and relatively less focus on the case of attractive extended interactions.

65 In this paper, we study the phase diagram of the extended Hubbard model on a square  
 66 lattice, for both attractive and repulsive nearest-neighbor interactions, using CDMFT+HFD,  
 67 an extension of the Cluster Dynamical Mean Field Theory (CDMFT) [100, 102] approach with  
 68 a Hartree-Fock decoupling of the inter-cluster interactions. CDMFT belongs to a class of meth-  
 69 ods called Quantum Cluster Methods [103–109]. This is a set of approaches that consider a  
 70 finite cluster of sites embedded in an infinite lattice, and introduce additional fields or “bath”  
 71 degrees of freedom, determined by variational or self-consistency principles, to best represent  
 72 the effect of the surrounding infinite lattice. These methods have proven useful for interpola-  
 73 tion between results obtained in the weak- and strong-coupling regimes, since their accuracy  
 74 is controlled by the size of the clusters used, rather than the strength of the couplings. Fur-  
 75 ther, we treat the inter-cluster interactions within a Hartree-Fock mean-field decoupling, which  
 76 generates additional Hartree, Fock and anomalous contributions to the cluster Hamiltonian.  
 77 While a similar treatment has been used to study the model at quarter-filling [48] for the case  
 78 of repulsive interactions, with the objective of understanding the electronic properties of met-  
 79 als close to a Coulomb-driven charge ordered insulator transition, this analysis was focused  
 80 on a specific parameter regime, and did not include superconducting orders.

81 This work constitutes a test of the CDMFT+HFD method, described in Sect. II below. Our  
 82 main findings are as follows. For a weak repulsive local interaction  $U$  and an attractive ex-  
 83 tended interaction  $V$ , the system undergoes a transition towards a phase separated (PS) state  
 84 when the chemical potential lies in the vicinity of its particle-hole symmetric value,  $U/2 + 4V$ .  
 85 The exact region of phase separation is identified by using the hysteresis in the behavior of the  
 86 electron density as a function of the chemical potential, which corresponds to the coexistence  
 87 of two different uniform-density solutions. As a function of doping away from the half-filled  
 88 point, symmetrical and sharply decaying regions of  $d_{x^2-y^2}$ -wave superconducting order are  
 89 observed, followed by disconnected pockets of extended  $s$ -wave order near quarter-filling, as  
 90 well as at very small (large) densities. A stronger attractive extended interaction tends to fa-  
 91 vor phase separation as well as superconductivity, whereas the repulsive on-site interaction  
 92  $U$  is found to be detrimental to both. At the particle-hole symmetric chemical potential, we  
 93 detect a first-order phase transition from antiferromagnetism (AF) to  $d$ -wave superconductiv-  
 94 ity as the attractive  $V$  becomes stronger, which is accompanied by a gradual deviation of the  
 95 density from its half-filled limit, induced by phase separation. For repulsive nearest-neighbor  
 96 interactions in the strong-coupling regime  $U \gg t$ , the Mott insulating state at half-filling is  
 97 destabilized, upon hole doping, in favor of a dome-shaped region of  $d$ -wave superconducting  
 98 order. This order is found to be remarkably stable in the presence of a non-local interaction,  
 99 and slightly suppressed by it. At half-filling, a repulsive non-local interaction induces a first-  
 100 order phase transition from antiferromagnetism (AF) to a charge-density wave (CDW) order.  
 101 Our results are qualitatively in agreement with the existing literature on the phase diagram  
 102 of the EHM, with some notable differences in the region of attractive interactions. An im-  
 103 portant difference is that intra-cluster fluctuations are treated exactly, which tends to make  
 104 superconducting orders somewhat weaker in this approach.

105 The paper is organized as follows. In Sect. II, we introduce the model Hamiltonian, and  
 106 provide a brief overview of the CDMFT approach that we use for our analysis, as well as the  
 107 Hartree-Fock mean-field decoupling of the intercluster interactions. In Sect. III, we describe  
 108 the phase diagram obtained as a function of the interaction strength and doping, and the phase

109 transitions observed at half-filling. Finally, in Sect. IV, we summarize our results, discuss some  
110 relevant observations and present the conclusions of our study.

## 111 2 Model and method

### 112 2.1 Model Hamiltonian

113 The general form of the extended Hubbard model Hamiltonian is

$$H = \sum_{\mathbf{r},\mathbf{r}',\sigma} t_{\mathbf{r}\mathbf{r}'} c_{\mathbf{r}\sigma}^\dagger c_{\mathbf{r}'\sigma} + U \sum_{\mathbf{r}} n_{\mathbf{r}\uparrow} n_{\mathbf{r}\downarrow} + \frac{1}{2} \sum_{\mathbf{r},\mathbf{r}',\sigma,\sigma'} V_{\mathbf{r}\mathbf{r}'} n_{\mathbf{r}\sigma} n_{\mathbf{r}'\sigma'} \quad (1)$$

114 where  $\mathbf{r}, \mathbf{r}'$  label lattice sites,  $t_{\mathbf{r}\mathbf{r}'}$  are the hopping amplitudes,  $U$  the on-site Hubbard interaction,  
115 and  $V_{\mathbf{r}\mathbf{r}'}$  the nearest-neighbor interaction (each bond counted once, hence the factor  $\frac{1}{2}$ ).

116 For the purpose of our analysis, we study the following model on a square lattice:

$$H = -t \sum_{\mathbf{r}} (c_{\mathbf{r}}^\dagger c_{\mathbf{r}+\mathbf{x}} + c_{\mathbf{r}}^\dagger c_{\mathbf{r}+\mathbf{y}} + \text{H.c.}) + U \sum_{\mathbf{r}} n_{\mathbf{r}\uparrow} n_{\mathbf{r}\downarrow} - \mu \sum_{\mathbf{r}} (n_{\mathbf{r}\uparrow} + n_{\mathbf{r}\downarrow}) + V \sum_{\mathbf{r},\sigma,\sigma'} (n_{\mathbf{r}\sigma} n_{\mathbf{r}+\mathbf{x},\sigma'} + n_{\mathbf{r}\sigma} n_{\mathbf{r}+\mathbf{y},\sigma'}) \quad (2)$$

117 where  $\mathbf{x}, \mathbf{y}$  are the lattice unit vectors along the  $x$  and  $y$  directions, and the operator  $c_{\mathbf{r}\alpha}$  an-  
118 nihilates a particle with spin  $\alpha = \uparrow, \downarrow$  at site  $\mathbf{r}$ . The occupation number is  $n_{\mathbf{r}\alpha} = c_{\mathbf{r}\alpha}^\dagger c_{\mathbf{r}\alpha}$ . We  
119 consider a range of values for the chemical potential  $\mu$ , corresponding to a continuous range  
120 of densities, from  $n = 0$  to  $2$ , along with a repulsive local interaction  $U > 0$ , and a nearest-  
121 neighbor interaction  $V$  that can be positive or negative. The particle-hole symmetric value of  
122 the chemical potential,  $\mu = U/2 + 4V$ , which corresponds to a half-filled band in the absence  
123 of phase separation, features prominently in our analysis. The unit of energy is taken to be  
124 the nearest-neighbor hopping amplitude  $t = 1.0$ , with the lattice constant  $a = 1$ . Note that  
125 in the absence of longer-range hopping terms, beyond the nearest-neighbor bonds, the model  
126 respects particle-hole symmetry  $n \rightarrow 2 - n$ .

127 We examine the possibility of superconducting as well as density-wave orders. For this  
128 purpose, the anomalous operators are defined on the lattice using a  $d$ -vector, as

$$\Delta_{\mathbf{r}\mathbf{r}',b} c_{\mathbf{r}\sigma} (i\sigma_b \sigma_2)_{\sigma\sigma'} c_{\mathbf{r}'\sigma'} + \text{H.c.} \quad (3)$$

129 where  $b = 0, 1, 2, 3$ , and  $\sigma_b$  are the Pauli matrices. The case  $b = 0$  corresponds to singlet  
130 superconductivity, in which case  $\Delta_{\mathbf{r}\mathbf{r}',0} = \Delta_{\mathbf{r}'\mathbf{r},0}$  and the cases  $b = 1, 2, 3$  correspond to triplet  
131 superconductivity, in which case,  $\Delta_{\mathbf{r}\mathbf{r}',b} = -\Delta_{\mathbf{r}'\mathbf{r},b}$ . In practice, these operators are defined by  
132 specifying  $b$  and the relative position  $\mathbf{r} - \mathbf{r}'$ .

133 Density wave operators are defined with a spatial modulation characterized by a wave  
134 vector  $\mathbf{Q}$ , and can be based on sites or on bonds. In our analysis, we focus on site density  
135 waves, defined as

$$\sum_{\mathbf{r}} A_{\mathbf{r}} \cos(\mathbf{Q} \cdot \mathbf{r} + \phi) \quad (4)$$

136 where  $A_{\mathbf{r}} = n_{\mathbf{r}}, S_{\mathbf{r}}^x, S_{\mathbf{r}}^z$  corresponds to charge- or spin-density wave orders, and  $\phi$  is a sliding  
137 phase. We probe the presence of density-wave orders with  $\mathbf{Q} = (\pi, \pi)$  and  $\phi = 0$ .

### 138 2.2 Method: CDMFT+HFD

139 Let us briefly describe the method used in our analysis, Cluster dynamical mean-field theory  
140 (CDMFT). For a detailed discussion of the basic principles of such Quantum Cluster Methods,  
141 please see Ref. [103, 105, 110].

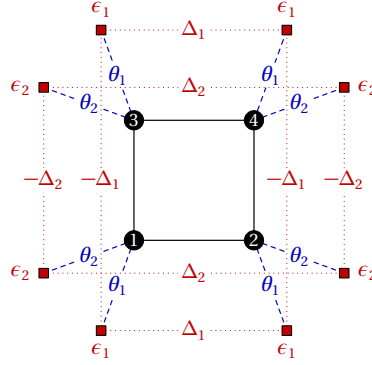


Figure 1: Schematic representation of the first (“simple”) impurity problem used in our analysis, with bath energies  $\epsilon_i$ , cluster-bath hybridization parameters  $\theta_i$  and anomalous bath parameters  $\Delta_i$ . Physical sites are marked by numbered black dots and bath orbitals by red squares. We choose the bath parameters such that the environment of each cluster site is identical. This impurity model has reflection symmetry with respect to horizontal and vertical mirror planes ( $C_{2v}$  symmetry), and typically involves only spin-independent hopping terms. Pairing terms  $\Delta_{1,2}$  are introduced between bath orbitals, with signs adapted to the SC order probed (shown here for a  $d$ -wave order, but all positive for an extended  $s$ -wave order). The number of independent bath parameters is 6.

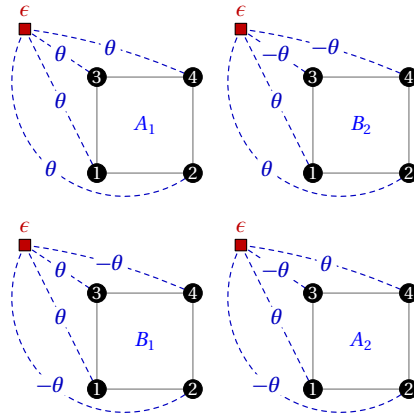


Figure 2: Schematic representation of the second (“general”) impurity problem used in our analysis. Each representation of the point group  $C_{2v}$  ( $A_{1,2}$  and  $B_{1,2}$ ) corresponds to a set of phases ( $\pm 1$ ), and each of the 8 bath orbitals belongs to one of these four representations (two bath orbitals per representation). The different bath orbitals are independent (the bath system is diagonal) and we only show here a view of each of the four representations with the corresponding signs associated to each cluster site (black dots). The hybridization parameters  $\theta$  are shown, and corresponding pairing operators (or anomalous hybridizations) between each bath orbital and each site also exist, with the same relative phases. The number of independent bath parameters is 18.

142 This approach is an extension of dynamical mean-field theory (DMFT) [111–114], which  
 143 accounts for short-range spatial correlations, by considering a cluster of sites with open bound-  
 144 ary conditions, instead of a single-site impurity. The effect of the cluster’s environment is taken  
 145 into account by introducing a set of uncorrelated “bath” orbitals hybridized with it. In this man-  
 146 ner, the infinite lattice is tiled into identical clusters coupled to a bath of auxiliary, uncorrelated  
 147 orbitals, with energy levels  $\epsilon_{i\sigma}$ , which may or may not be spin dependent, and hybridized with  
 148 the cluster sites (labeled  $r$ ) with amplitudes  $\theta_{ir\sigma}$ . In addition, for studying superconducting  
 149 orders, different types of anomalous pairings  $\Delta_{ij\sigma\sigma'}$  may be introduced between bath orbitals  
 150  $i, j$  or  $\Delta_{ir\sigma\sigma'}$  between bath orbital  $i$  and cluster site  $r$ .

151 In our analysis, we use two types of bath models. In the simple model (Fig. 1), the environ-  
 152 ment of each cluster is identical, and we introduce two bath orbitals per cluster site. Param-  
 153 eters of the impurity model include bath orbital energy levels ( $\epsilon_{1,2}$ ), hybridization between  
 154 each cluster site and the corresponding bath orbitals ( $\theta_{1,2}$ ), and pairings between the bath  
 155 orbitals ( $\Delta_{1,2}$ ). The precise form of  $\Delta_{1,2}$ , including their relative phases between different  
 156 bath orbitals, depends on whether we probe extended  $s$ -wave,  $d$ -wave, or triplet supercon-  
 157 ductivity. This simple impurity model involves 6 independent parameters to be determined  
 158 self-consistently. At half-filling, we introduce bath energies as well as hoppings, that are con-  
 159 sistent with the appearance of a density-wave order, and additionally spin-dependent in the  
 160 presence of antiferromagnetism. This increases the number of independent parameters. How-  
 161 ever, imposing particle-hole symmetry at half-filling once again reduces this number to 6.

162 We also use a more general bath model (Fig. 2). While the total number of bath orbitals  
 163 is unchanged, every bath orbital is connected to every cluster site (with distinct combinations  
 164 of relative phases), and we define bath energies, cluster-bath hybridizations and anomalous  
 165 pairings between the cluster and the bath sites. In this model the bath is diagonal, i.e., the  
 166 different bath orbitals are not directly coupled between themselves, and, taking into account  
 167 rotation symmetry, there are 18 independent bath parameters to set. At the particle-hole sym-  
 168 metric chemical potential, we introduce bath energies, hybridizations and anomalous pairings  
 169 that have two different values for alternative sites. Even upon taking into account particle-hole  
 170 symmetry, this gives us a total of 52 independent parameters in the presence of superconduc-  
 171 tivity, and 20 independent parameters when superconductivity is absent (i.e. for  $V > 0$ ).

172 All bath parameters are determined by a self-consistency condition (see Ref. [103, 105, 110]  
 173 for details). The simple bath model is expected to be easier to converge than the general bath  
 174 model, because of the smaller set of parameters. While we expect the results obtained from the  
 175 general bath model to be more reliable, we do find most of the results to be qualitatively similar  
 176 in the two cases. Once the bath parameters are converged, the self-energy  $\Sigma(\omega)$  associated  
 177 with the cluster is applied to the whole lattice, so that the lattice Green function is

$$\mathbf{G}^{-1}(\tilde{\mathbf{k}}, \omega) = \mathbf{G}_0^{-1}(\tilde{\mathbf{k}}, \omega) - \Sigma(\omega) \quad (5)$$

178 Here,  $\tilde{\mathbf{k}}$  denotes a reduced wave vector (defined in the Brillouin zone of the super-lattice  
 179 of clusters defined by the tiling) and  $\mathbf{G}_0$  is the non-interacting Green function. The Green-  
 180 function-like objects  $\mathbf{G}$ ,  $\mathbf{G}_0$  and  $\Sigma$  are  $L \times L$  matrices,  $L$  being the number of physical degrees  
 181 of freedom on the cluster (here  $L = 8$  because of spin and the four cluster sites). The aver-  
 182 age values of one-body operators defined on the lattice are obtained using the lattice Green  
 183 function  $\mathbf{G}$  determined from the solution for the optimum values of the bath parameters. An  
 184 exact-diagonalization solver (the Lanczos method or variants thereof) is used at zero temper-  
 185 ature. The computational size of the problem increases exponentially with the total number  
 186 of cluster and bath orbitals.

187 In the presence of extended interactions, we also perform a Hartree-Fock mean-field de-  
 188 composition of the interaction terms defined between different clusters, while the interactions  
 189 within a cluster are treated exactly. The inter-cluster interactions are decoupled in the Hartree,

190 Fock and anomalous channels, which contribute to the number density, the hopping and the  
 191 pairing operators, respectively. Moreover, we only retain those combinations of the site/bond  
 192 operators that are physically relevant in the regions we work in (such as  $d$ -wave or extended  
 193  $s$ -wave), and discard the rest. The mean-field values of the relevant combinations are deter-  
 194 mined self-consistently, within the CDMFT loop that optimizes the bath parameters. For the  
 195 details of this procedure, please refer to the Appendix.

## 196 3 Results

197 In this section, we discuss the salient features of the phase diagram obtained from our analysis,  
 198 for both attractive and repulsive nearest-neighbor interactions. The dominant superconduct-  
 199 ing and density-wave orders are identified by computing the corresponding order parameters  
 200 using the optimum values of the CDMFT (bath and mean-field) parameters, as a function of  
 201 electron density, as well as at half-filling. In the following analysis, we focus our attention on  
 202 the strong coupling limit  $U \gg t$  for  $V > 0$ , which is a regime well-understood on physical  
 203 grounds. For  $V < 0$ , we consider relatively weak interactions  $U \sim t$ , far from the Mott insu-  
 204 lating regime, which primarily serve the purpose of controlling the extent of phase separation  
 205 when the interaction  $V$  becomes sufficiently attractive. At half-filling, we confirm the nature  
 206 of the phase transitions, by plotting the relevant order parameters both as a function of  $U > 0$ ,  
 207 for fixed values of  $V > 0$  or  $V < 0$ , and as a function of  $V$  for fixed values of  $U$ .

### 208 3.1 Phase diagram at the particle-hole symmetric chemical potential

209 Here, we fix the chemical potential to  $\mu = U/2 + 4V$ , corresponding to a half-filled band, and  
 210 examine the behavior of different superconducting and density-wave orders, as a function of  
 211 the local repulsion  $U$  as well as attractive/repulsive  $V$ . While antiferromagnetism is favored at  
 212 half-filling, in both the weak- and strong-coupling regimes, an attractive non-local interaction  
 213 is expected to drive the system towards a superconducting instability, and eventually phase  
 214 separation. On the other hand, repulsive interactions  $V$  would typically foster competition  
 215 between charge and spin fluctuations, and favor a charge-ordered state. Below, we discuss the  
 216 results obtained using the simple bath model (Fig. 1).

#### 217 3.1.1 $V < 0$ :

218 For a fixed attractive nearest-neighbor interaction  $V$ , as the strength of the local repulsive  
 219 interaction  $U$  decreases, the system undergoes a first-order phase transition from antiferro-  
 220 magnetism to  $d$ -wave superconductivity. This is accompanied by a deviation in the electron  
 221 density from its half-filled limit, which can be attributed to the effects of phase separation, dis-  
 222 cussed in more detail in the next subsection. Each of the order parameters is plotted for both  
 223 increasing and decreasing  $U$ , and the region of hysteresis between the two curves indicates  
 224 that the transition is first-order in nature. We have verified that other pairing symmetries,  
 225 such as extended  $s$ -wave and  $p$ -wave, do not compete with  $d_{x^2-y^2}$  pairing in this regime. The  
 226 results of our analysis are shown in Fig. 3. Likewise, an antiferromagnetic order is destabilized  
 227 in favor of  $d$ -wave superconductivity for an attractive  $V$ , at a fixed repulsive  $U \sim t$ , with sig-  
 228 nificant hysteresis between the curves obtained for increasing/decreasing  $V$ . The latter state is  
 229 then rapidly suppressed due to the effect of phase separation. The results are shown in Fig. 4.

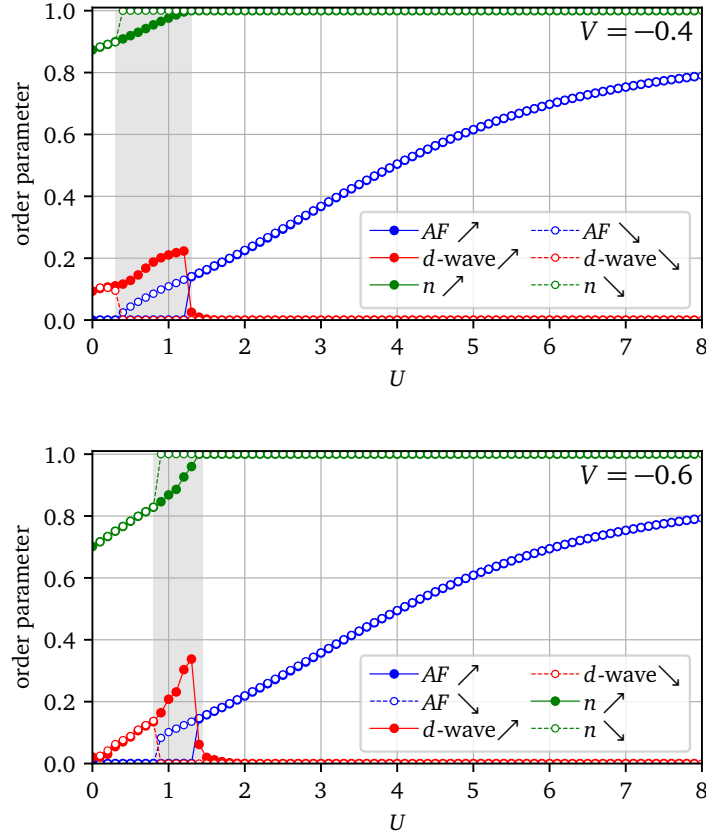


Figure 3: First-order phase transition from  $d$ -wave superconductivity (indicated by filled/open red circles) to antiferromagnetism (AF, indicated by filled/open blue circles), as a function of the repulsive local interaction  $U$ , at fixed  $V = -0.4$  (top) and  $V = -0.6$  (bottom), and fixed chemical potential  $\mu = U/2 + 4V$  (particle-hole symmetric point). The simple impurity model (Fig. 1) is used. The transition is accompanied by a deviation in the number density (indicated by filled/open green circles) from the half-filled value  $n = 1$ , meaning that we are entering a phase separated regime. This may also explain the rapid suppression of superconductivity for smaller values of  $U$  for a more negative interaction  $V$ . The dashed (solid) curves of each color depict the behavior of the different quantities for decreasing (increasing)  $U$ , respectively. The prominent region of hysteresis between the two curves confirms the order of the transition.



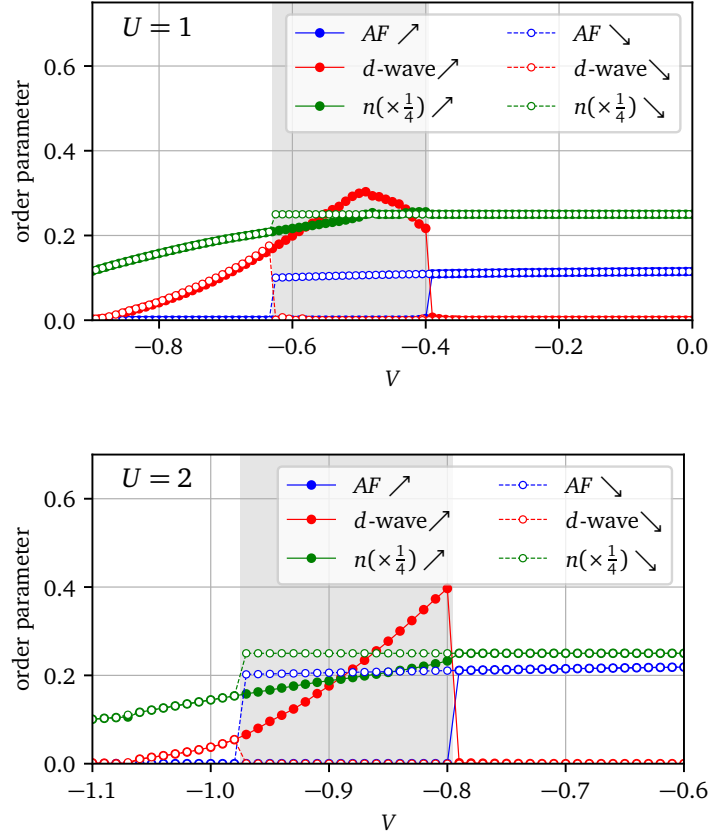


Figure 4: First-order phase transition from antiferromagnetism (AF) (indicated by filled/open blue circles) to  $d$ -wave superconductivity (indicated by filled/open red circles), for increasingly attractive  $V$ , followed by a rapid suppression in the superconducting order parameter, for on-site interaction  $U = 1$  (top) and  $U = 2$  (bottom). The simple impurity model (Fig. 1) is used. The transition is accompanied by a deviation in the number density (indicated by filled/open green circles) from the half-filled value  $n = 1$ . The dashed (solid) curves of each color depict the behavior of different quantities for decreasing/more negative (increasing/less negative)  $V$ , and we find significant hysteresis. For larger repulsive interactions  $U$ , the transition is found to occur at a critical value of  $V$  that is more attractive.

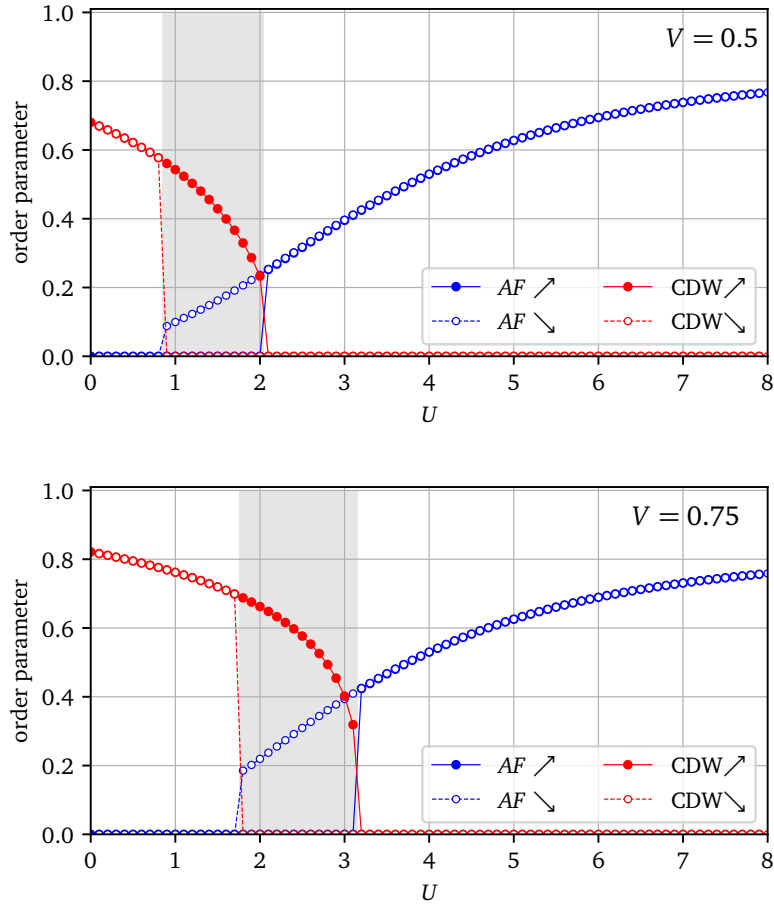


Figure 5: First-order phase transition from a charge-density wave (CDW) order (indicated by filled/open red circles) to antiferromagnetism (indicated by filled/open blue circles), at half-filling, as a function of the local repulsive interaction  $U$ , for  $V = 0.5$  (top) and  $V = 0.75$  (bottom). The simple impurity model (Fig. 1) is used. The dashed (solid) curves of each color depict the behavior of the order parameters for decreasing (increasing)  $U$ , and exhibit significant hysteresis. As the repulsive  $V$  becomes stronger, the transition is found to occur at a larger value of  $U$ , the CDW order parameter increases considerably in magnitude, and the region of hysteresis is somewhat enhanced.

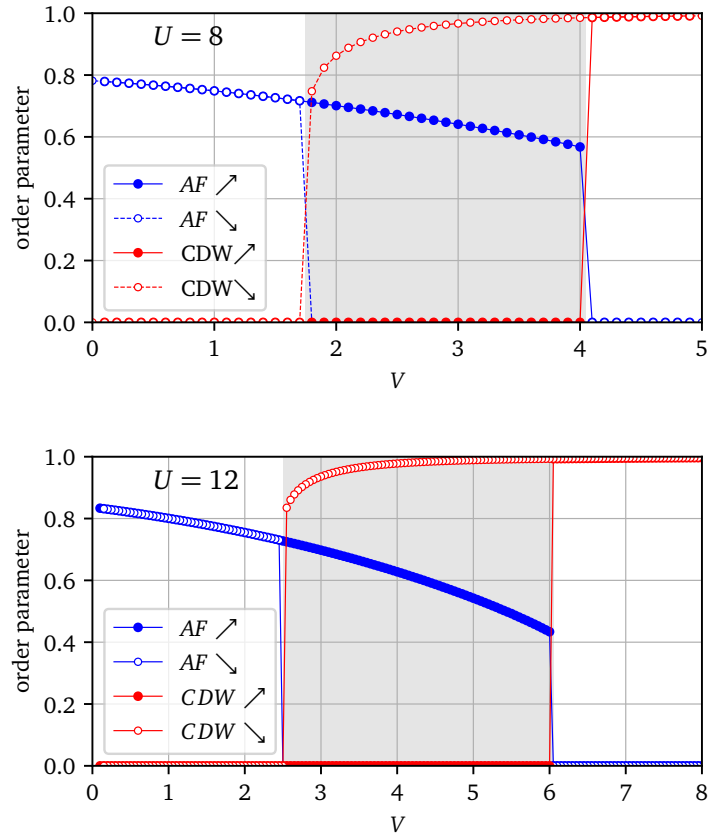


Figure 6: First-order phase transition from antiferromagnetism (indicated by filled/open blue circles) to charge-density wave (CDW) order (indicated by filled/open red circles), at half-filling, as a function of the repulsive interaction  $V$  for fixed  $U$ , with  $U = 8$  (top) and  $U = 12$  (bottom). The simple impurity model (Fig. 1) is used. The dashed (solid) curves of each color depict the behavior of the order parameters for decreasing (increasing)  $V$ , and exhibit considerable hysteresis. As  $U$  increases, the transition occurs at a larger critical value of  $V$ , and the antiferromagnetic order parameter increases in magnitude.

### 230 3.1.2 $V > 0$ :

231 For repulsive nearest-neighbor interactions  $V$ , we do not expect to find any superconducting  
 232 orders at half-filling in the strong-coupling limit  $U \gg t$ , and instead focus on studying the  
 233 competition between charge- and spin-density-wave orders. At fixed  $V > 0$ , we observe a  
 234 first-order phase transition from a charge-density wave (CDW) to an antiferromagnetic (AF)  
 235 state, as a function of increasing  $U$ . Likewise, for a large repulsive  $U$ , the system undergoes  
 236 a phase transition from antiferromagnetism to CDW, as a function of the repulsive  $V$ . In both  
 237 cases, a large region of hysteresis is observed between the results obtained for increasing and  
 238 decreasing values of the respective interaction couplings. The results of our analysis are shown  
 239 in Figs 5 and 6, respectively.

240 We do not present the corresponding results for the more general bath model (Fig. 2) here,  
 241 as they are found to be qualitatively similar to those obtained for the simple model. The key  
 242 differences, that are sometimes observed, include a) an increase/decrease in the strength of  
 243 the  $d$ -wave order parameter close to the transition, b) a smaller region of hysteresis, c) a  
 244 small shift in the position of the transition, particularly as a function of  $V$  for fixed  $U$ .

## 245 3.2 Phase diagram as a function of density

246 Next, we examine the phase diagram of the model over a continuous range of densities, for  
 247  $U > 0$  and attractive/repulsive  $V$ . For  $V > 0$ , we once again limit ourselves to the strong-  
 248 coupling limit  $U \gg t$ . For  $V < 0$ , we focus on studying the effect of an attractive extended  
 249 interaction, with a local repulsion  $U$  controlling the extent of phase separation.

### 250 3.2.1 $V < 0$ :

251 Let us now discuss the different phases that are supported by the model as a function of den-  
 252 sity. Close to half-filling, we find a region of phase separation, indicated by a jump in the  
 253 density, flanked by symmetrical pockets of  $d_{x^2-y^2}$  pairing, which decay rapidly as a function  
 254 of density. For further smaller (larger) fillings, an extended  $s$ -wave order appears in the form  
 255 of disconnected patches, near quarter-filling and at very small (large) densities. Interestingly,  
 256 the variation of the extended  $s$ -wave order parameter as a function of  $U$  and  $V$  are found  
 257 to be different for the simple bath model and the more general one. In the case of the sim-  
 258 ple model (see Fig. 7), we find small regions of extended  $s$ -wave superconductivity near  
 259 quarter-filling, that vary non-monotonously as a function of  $U$ . Only for sufficiently attractive  
 260  $V$ , nearly symmetrical patches of extended  $s$ -wave order also appear close to the band edges.  
 261 The corresponding results for the general bath model are illustrated in Fig. 8. While the over-  
 262 all magnitude of the  $s$ -wave order parameter turns out to be smaller than in the previous case,  
 263 its shape is more extended at quarter-filling, with two patches appearing next to each other,  
 264 which, interestingly, appear close to fillings of  $1/3$  and  $1/2$ , respectively. While it is tempting  
 265 to blame the  $n = 1/2$  feature on a commensurate finite-size effect on a 4-site cluster, this is  
 266 less obvious for the  $n = 1/3$  feature. The superconductivity also clearly becomes stronger as  
 267 a function of  $V < 0$ . Notably, the  $s$ -wave order is clearly absent for both  $U = 1$  and  $U = 2$ ,  
 268 thus eliminating the confusion caused by the aforementioned non-monotonous variation in  
 269 the case of the simple model.

270 To better characterize the region of phase separation, we examine the behavior of the num-  
 271 ber density  $n$  as a function of the chemical potential  $\mu$ , measured with respect to its particle-  
 272 hole symmetric value  $\mu_c = U/2 + 4V$ . On either side of  $\mu = \mu_c$ , we find symmetrical jumps  
 273 in the compressibility  $\partial n / \partial \mu$ , enclosing a region of hysteresis in the  $\mu - n$  curve, depicted in  
 274 Fig. 9, where two uniform-density solutions coexist. Within our approach, this is interpreted  
 275 as the region of phase separation, and is found to shrink under the influence of stronger local

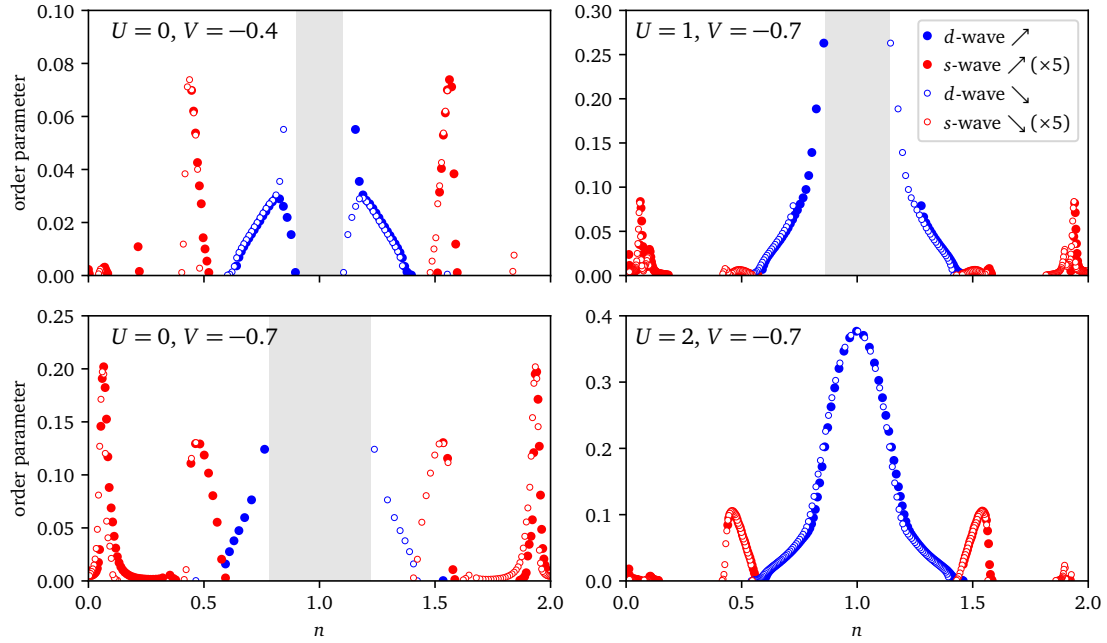


Figure 7: Superconducting order parameter of the EHM with attractive nearest-neighbor interactions, as a function of density  $n$ , from  $n = 0$  to 2 for the simple bath model (Fig. 1). Close to the half-filled value  $n = 1$ , we find signatures of phase separation, indicated by a gap in the curve over a range of densities, caused by a jump in the compressibility  $\partial n / \partial \mu$  (as shown in Fig. 9). For smaller (larger) fillings, symmetrical and sharply defined regions of  $d$ -wave superconductivity (represented by filled/open blue circles) are followed by disconnected patches of extended  $s$ -wave order (represented by filled/open red circles), which appear only beyond a critical attractive value of  $V$ .

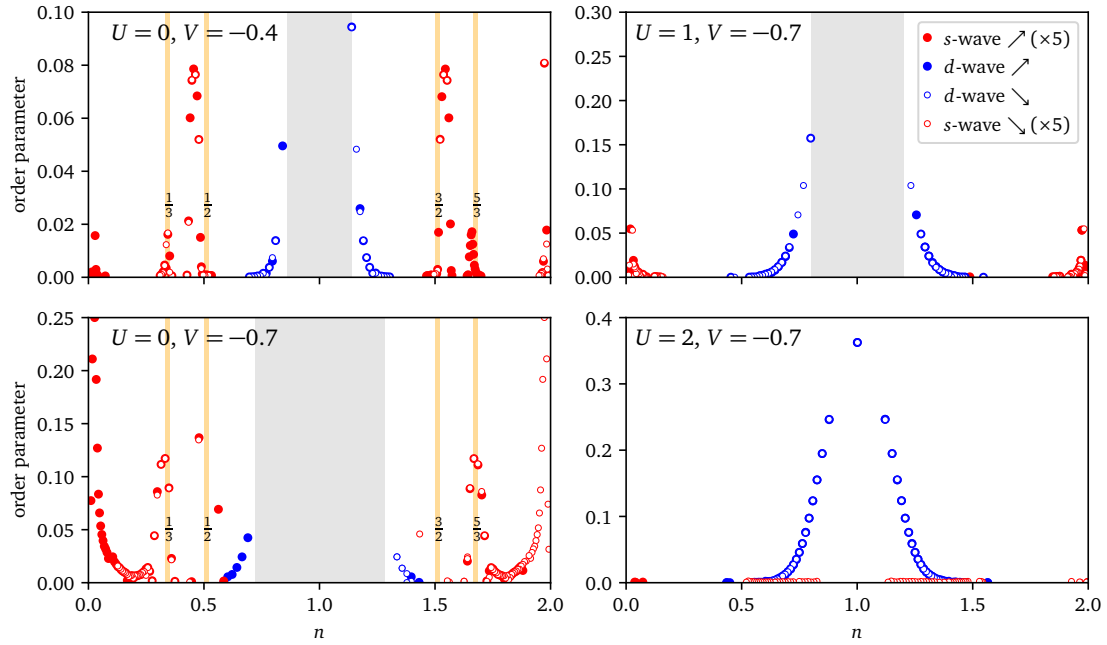


Figure 8: Superconducting order parameter of the EHM with attractive nearest-neighbor interactions, as a function of density  $n$ , from  $n = 0$  to 2 for the general bath model (Fig. 2). The overall behavior of the  $d$ - and extended  $s$ -wave patches are similar to the corresponding result for the simple bath model. However, note that the structure of the  $s$ -wave order parameter has changed, with a more extended region near quarter-filling, and an additional patch near  $1/3$ -filling. For  $U = 0, V = -0.7$ , the phase separation region extends all the way to quarter-filling, and the corresponding superconducting patches are almost absent, and asymmetric about  $n = 1$ . Moreover, the new  $s$ -wave order parameter becomes unambiguously weaker as the repulsive  $U$  increases, and is completely absent for  $U = 1$  and  $U = 2$ , thus resolving the question of the nonmonotonous behavior of the  $s$ -wave order parameter in the simple bath model.

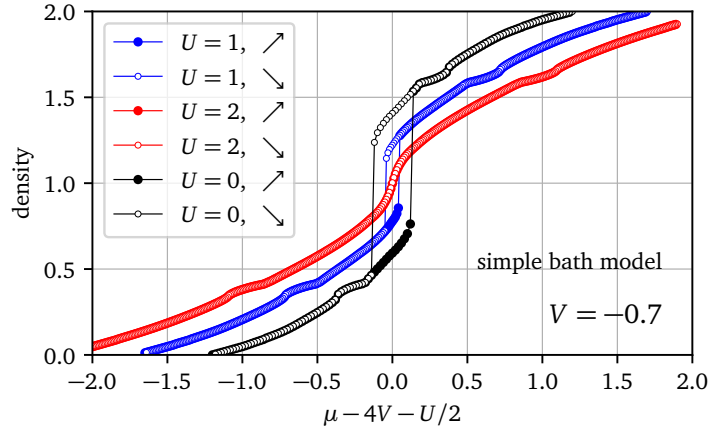


Figure 9: Number density  $n$  as a function of the chemical potential  $\mu$  (measured with respect to its particle-hole invariant value,  $\mu_c = U/2 + 4V$ ) for an EHM with attractive nearest-neighbor interactions, over a range of values of  $U \geq 0$  and  $V < 0$  for the simple bath model (Fig. 1). On either side of half-filling ( $\mu = \mu_c$ ), we find symmetrical jumps in the compressibility  $\partial n / \partial \mu$  enclosing a region of hysteresis, which corresponds to the coexistence of two different uniform-density solutions. This is interpreted as the region of phase separation. The red, blue and black filled/open circles represent the behavior for various values of  $U$  for  $V = -0.7$ , and demonstrate that while a sufficiently attractive interaction  $V$  favors phase separation, a stronger on-site repulsion  $U$  is detrimental to it.

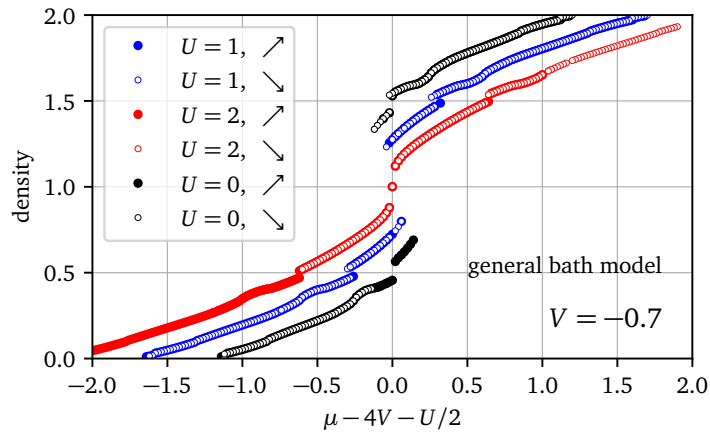


Figure 10: Number density  $n$  as a function of the chemical potential  $\mu$  (measured with respect to its particle-hole invariant value,  $\mu_c = U/2 + 4V$ ) for the EHM with attractive nearest-neighbor interactions, over a range of values of  $U \geq 0$  and  $V < 0$  for the general bath model (Fig. 2). The behavior is very similar to that observed in the simple bath model, with the most notable difference being the appearance of symmetric jumps in the number density  $n$ , close to quarter-filling, for each of the curves.

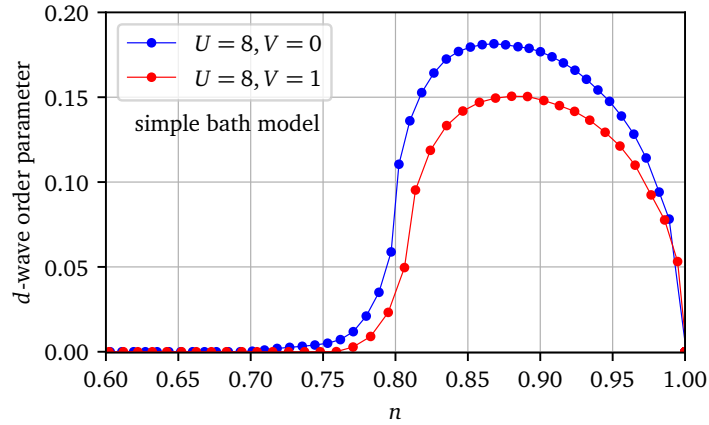


Figure 11: Superconducting  $d$ -wave order parameter of the EHM with repulsive nearest-neighbor interactions in the strong-coupling limit, i.e., at  $U = 8t$ , using the simple bath model (Fig. 1). The Mott insulating state at half-filling is destabilized in favor of  $d_{x^2-y^2}$  pairing, upon hole doping. The dome-like region of  $d$ -wave superconducting order is observed for  $V = 0$  (indicated by the solid blue curve) and is somewhat suppressed for non-zero repulsive  $V$  (indicated by the solid red curve). No other superconducting orders are found to be stabilized in this region.

276 repulsive interactions  $U$ , and expand when  $V$  becomes more attractive. The corresponding re-  
 277 sults for the general bath model are depicted in Fig. 10. The two sets of results are qualitatively  
 278 similar, except for symmetric jumps observed in the number density  $n$  near quarter-filling in  
 279 the latter case. We note that the jumps occur only for the model with the larger number of  
 280 bath parameters, and are the most prominent for  $U = 0, V = -0.7$ , where the phase separa-  
 281 tion region extends all the way to quarter-filling, becoming progressively smaller for  $U = 1$   
 282 and 2. It is plausible that phase separation might lead to the appearance of multiple jumps in  
 283 the density, at half-filling as well as quarter-filling. Moreover, a finite-size effect would have  
 284 been even more obvious in the simple bath model, where these jumps are found to be absent.  
 285 The origin of the jumps is currently unclear to us.

286 The appearance of a phase separated state for sufficiently attractive interactions is a famil-  
 287 iar result [32, 52, 71, 81, 87, 115], which has received attention from other groups, including  
 288 very recently [70], but the characterization of the region of phase separation tends to depend  
 289 on the method used for the analysis, and whether it is capable of handling a non-uniform  
 290 distribution of particles.

### 291 3.2.2 $V > 0$ :

292 At half-filling, for  $U = 8t$ , the large on-site interaction freezes the charge degree of freedom,  
 293 and the ground state is a Mott insulator. Hole doping is found to destabilize the magnetic  
 294 order, and drive the system towards a  $d$ -wave superconducting phase. We encounter a dome-  
 295 shaped region of  $d$ -wave superconductivity for  $V = 0$ , which is suppressed at smaller densities,  
 296 where no competing superconducting orders are found to be stabilized in our analysis. Upon  
 297 introducing a repulsive  $V \sim t$ , the superconducting order remains stable, but is somewhat  
 298 suppressed. The results are depicted in Fig. 11. The corresponding results for the general bath  
 299 model are depicted in Fig. 12. The two sets of results are qualitatively similar, with the most  
 300 noticeable difference being the relatively sharper transition to and from the  $d$ -wave ordered  
 301 state in the latter case. These results are consistent with the picture of superconductivity



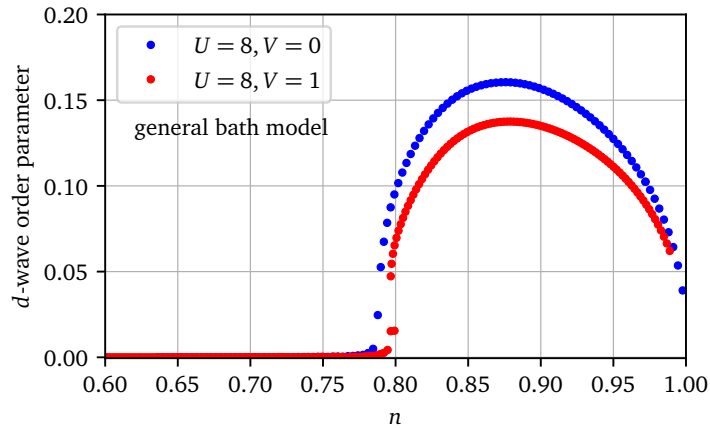


Figure 12: Superconducting  $d$ -wave order parameter of the EHM with repulsive nearest-neighbor interactions in the strong-coupling limit ( $U = 8t$ ) using the general bath model (Fig. 2). The behavior is qualitatively similar to that obtained in the simple model, with a slight difference in the magnitudes of the  $d$ -wave order parameter. The most noticeable difference between the two bath models is the relatively sharp transition into and out of the  $d$ -wave superconducting phase.

302 mediated by short-range spin fluctuations in a doped Mott insulator [116–118].

## 303 4 Discussion and conclusions

304 In summary, we have studied the phase diagram of the extended Hubbard model, for both  
 305 attractive and repulsive nearest-neighbor interactions, using a combination of Cluster Dynamical  
 306 Mean Field Theory (CDMFT), with a dynamical Hartree-Fock approximation for treating  
 307 inter-cluster interactions. We examine possible phase transitions at half-filling, as well as the  
 308 dominant phases that are stabilized as a function of density. At the particle-hole invariant  
 309 chemical potential, which corresponds to a half-filled band in the absence of phase separation,  
 310 the antiferromagnetically ordered state undergoes a first-order phase transition to  $d$ -wave su-  
 311 perconductivity for a critical attractive interaction  $V$ . Stronger attractive extended interactions  
 312 also tend to induce phase separation, which manifests itself in the form of a gradual deviation  
 313 of the density from its half-filled limit, for a fixed chemical potential. For a sufficiently strong  
 314 repulsive interaction  $V$ , a charge-density wave order is stabilized at half-filling. As a function  
 315 of density, a phase separated state near the half-filled point is flanked by symmetrical regions  
 316 of  $d$ -wave superconductivity, that decay sharply as a function of density, and disconnected  
 317 patches of extended  $s$ -wave order at smaller (larger) band fillings. For the case of repulsive  
 318 non-local interactions, in the strongly coupled limit, the Mott insulator at half-filling gives way  
 319 to a dome-shaped region of  $d$ -wave superconductivity, upon hole doping, which is expected  
 320 on physical grounds. No other competing superconducting orders are found to be stabilized  
 321 in this region of parameter space.

322 For the most part, our results are found to be qualitatively consistent with the existing  
 323 literature. The transition between antiferromagnetism and CDW at half-filling, for repulsive  
 324 interactions, has been predicted by several previous studies [26,31,54,58,62,65,70,76–78,87],  
 325 although the critical interaction strength typically depends on the method of analysis. For  
 326 densities away from half-filling, there have also been some predictions of  $d_{xy}$  pairing, that  
 327 appears beyond the region of  $d_{x^2-y^2}$  pairing, for repulsive extended interactions [39,56]. We

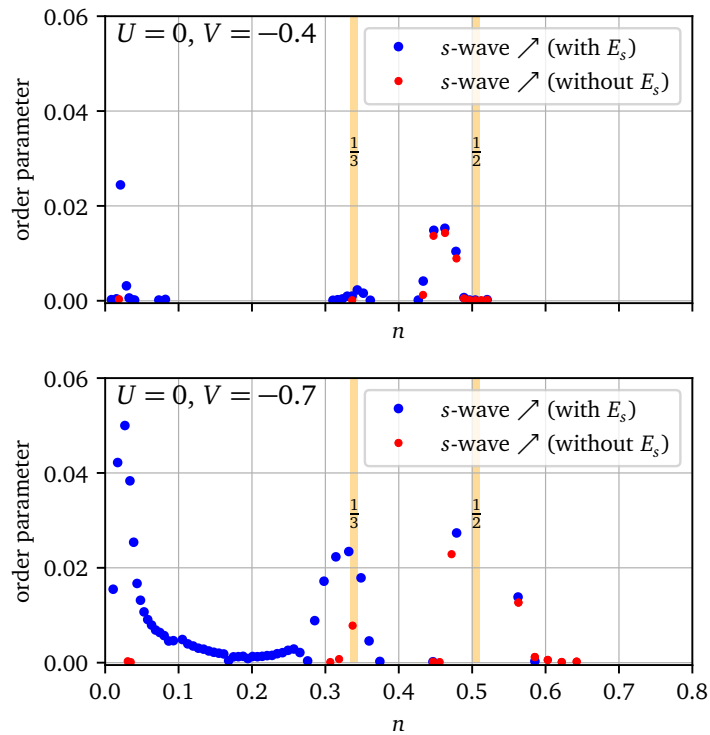


Figure 13: The figure shows the behavior of the extended  $s$ -wave order parameter as a function of the number density  $n$ , with and without the inclusion of the self-consistent anomalous mean-field parameter  $E_s$  (see Appendix), for  $U = 0, V = -0.4$  (above) and  $U = 0, V = -0.7$  (below). Clearly, some of the regions with a nontrivial  $s$ -wave order parameter are found to be absent when  $E_s$  is not included. Upon considering a stronger attractive  $V$ , these regions tend to reappear, but are suppressed in magnitude in the absence of  $E_s$ .

328 do not find such a state in our analysis. The phase diagrams obtained from self-consistent  
329 mean-field theory based analyses tend to prominently feature  $d$ -wave superconductivity at  
330 half-filling, with a continuous region of extended  $s$ -wave order at smaller densities, along with  
331 a region of coexistence between the two, i.e.,  $s + id$  pairing [50, 51]. In our analysis, we do  
332 not usually see a coexistence between  $d$ - and extended  $s$ -wave orders. In the simple model,  
333 such a coexistence is observed only in those regimes where both the interactions  $U > 0$  and  
334  $V < 0$  are sufficiently strong, and comparable in magnitude. This may be due to the fact  
335 that the superconducting orders found in our analysis are fairly weak, and the significant  
336 attractive interactions that are, therefore, needed for stabilizing overlapping regions of  $d$ -  
337 and extended  $s$ -wave orders, would also lead to a larger region of phase separation. This  
338 effect can only be compensated by including a sufficiently large repulsive local interaction.  
339 On the other hand, we have not been able to verify a similar coexistence of the orders for  
340 the general bath model, due to the rapid suppression of the extended  $s$ -wave order, near  
341 quarter-filling, with an increase in  $U$ . Some studies have also suggested the possibility of  
342  $p$ -wave superconductivity, especially at half-filling [32], and for intermediate hole doping,  
343 beyond the region of  $d$ -wave superconducting order [39, 50, 51]. We do not find signatures of  
344  $p$ -wave superconductivity in the parameter regimes that we study. Some of our results at half-  
345 filling are found to be qualitatively consistent with a recent study on the extended Hubbard  
346 model using the determinantal Quantum Monte Carlo technique [70], which also reports the  
347 transitions between  $d$ -wave superconductivity and AFM, as well as between phase separation  
348 and  $d$ -wave, that we observe in our analysis. In addition, the authors of the aforementioned  
349 paper also explore other quadrants of the  $U - V$  phase diagram, including the case where  
350  $U < 0$ , which we do not take into account, since the repulsive component of the Coulomb  
351 interaction is always expected to be present in a realistic situation.

352 In contrast to ordinary mean-field theory, our approach takes the intra-cluster fluctuations  
353 into account exactly, and is therefore expected to give more reliable quantitative results. In par-  
354 ticular, ordered phases are weaker in this approach than in ordinary mean-field theory. At the  
355 same time, it should be noted that we only take into account spatial fluctuations within small  
356 clusters, and the accuracy of the method is controlled by the size of the clusters used. To illus-  
357 trate the importance of including the effect of the inter-cluster interactions self-consistently,  
358 which are usually disregarded in cluster-based approaches, we have compared the behavior  
359 of the superconducting  $d$ - and extended  $s$ -wave orders as a function of density  $n$ , for an at-  
360 tractive  $V$  (see Fig. 13) in the presence and absence of the anomalous mean-field parameters  
361 (which we refer to as  $E_d$  and  $E_s$  respectively). Certain regions of the extended  $s$ -wave order,  
362 that we observe in our analysis, disappear entirely in the absence of the self-consistent anoma-  
363 lous mean field parameter  $E_s$ . These regions tend to reappear, but with a smaller amplitude,  
364 when the attractive  $V$  is sufficiently strong. Likewise, in the case of  $d$ -wave superconduc-  
365 tivity, we find that the superconducting order parameter is negligible when  $E_d$  is absent, and  
366 tends to reappear, with a much smaller amplitude, when the repulsive  $U$  is increased. Our  
367 approach is more suitable for making predictions about the thermodynamic limit than exact  
368 diagonalization studies on finite-sized clusters, since only the self-energy is limited by the  
369 cluster size. Some recent studies have explored the possibility of magnetic states character-  
370 ized by ordering wave vectors that are incommensurate with the lattice periodicity [119] in  
371 the two-dimensional Hubbard model, for electron densities below half-filling, where the anti-  
372 ferromagnetic state becomes unstable. Our approach is unsuitable for identifying such incom-  
373 mensurate charge and spin orders. Our method does not suffer from fundamental restrictions  
374 on its applicability in any particular parameter regime, and allows us to study the behavior of  
375 the model as a continuous function of doping, rather than by focusing on specific densities, as  
376 has been done in many previous studies. In the future, this method could be potentially useful  
377 for analysing more complicated models, including those with spin-orbit interactions.

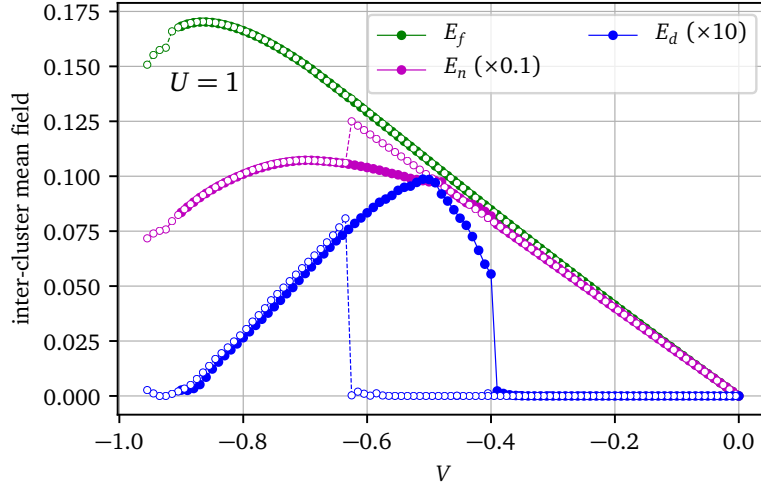


Figure 14: Inter-cluster Hartree-Fock mean fields for the solutions shown in the top panel of Fig. 4.  $E_d$  is the eigen-operator associated with  $d$ -wave superconductivity,  $E_f$  with the nearest-neighbor kinetic operator  $f_{\mathbf{r}\mathbf{r}'\sigma\sigma}$  and  $E_n$  with the density  $n$  (basically a shift in the chemical potential induced by  $V$ ). The mean-field  $E_s$  associated with extended  $s$ -wave superconductivity is negligible over almost the entire range of  $V$ , since this is at half-filling, except at significantly attractive  $V$  (due to phase separation). Note the very different scales (the superconducting mean field is much magnified). The filled and empty circles denote the results for increasing (less negative) and decreasing (more negative)  $V$ , respectively.

378 **Funding information** S.K. acknowledges financial support from the Postdoctoral Fellowship  
 379 from Institut Quantique, and from UF Project No. P0224175 - Dirac postdoc fellowship, spon-  
 380 sored by the Florida State University National High Magnetic Field Laboratory (NHMFL). D.S.  
 381 acknowledges support by the Natural Sciences and Engineering Research Council of Canada  
 382 (NSERC) under grant RGPIN-2020-05060. Computational resources were provided by the  
 383 Digital Research Alliance of Canada and Calcul Québec.

## 384 A Appendix

385 The extended interaction term can be rewritten as

$$\frac{1}{2} \sum_{\mathbf{r}, \mathbf{r}', \sigma, \sigma'} V_{\mathbf{r}\mathbf{r}'} n_{\mathbf{r}\sigma} n_{\mathbf{r}'\sigma'} = \frac{1}{2} \sum_{\mathbf{r}, \mathbf{r}', \sigma, \sigma'} V_{\mathbf{r}\mathbf{r}'}^c n_{\mathbf{r}\sigma} n_{\mathbf{r}'\sigma'} + \frac{1}{2} \sum_{\mathbf{r}, \mathbf{r}', \sigma, \sigma'} V_{\mathbf{r}\mathbf{r}'}^{\text{ic}} n_{\mathbf{r}\sigma} n_{\mathbf{r}'\sigma'}$$

386 where  $\mathbf{r}, \mathbf{r}'$  refer to the lattice sites, and  $n_{\mathbf{r}\sigma}$  is the number of particles at site  $\mathbf{r}$  with spin  $\sigma$ .  
 387 Here  $V_{\mathbf{r}\mathbf{r}'}^c$  and  $V_{\mathbf{r}\mathbf{r}'}^{\text{ic}}$  refer to the intra-cluster and inter-cluster parts of the interaction. Inspired  
 388 by Wick's theorem, we decompose the inter-cluster part of the interaction into Hartree, Fock

389 and anomalous channels, as follows:

$$\begin{aligned}
\frac{1}{2} \sum_{\mathbf{r}, \mathbf{r}', \sigma, \sigma'} V_{\mathbf{r}\mathbf{r}'}^{\text{ic}} n_{\mathbf{r}\sigma} n_{\mathbf{r}'\sigma'} &= \sum_{\mathbf{r}, \mathbf{r}', \sigma, \sigma'} V_{\mathbf{r}\mathbf{r}'}^{\text{ic}} \left( n_{\mathbf{r}\sigma} \bar{n}_{\mathbf{r}'\sigma'} - \frac{1}{2} \bar{n}_{\mathbf{r}\sigma} \bar{n}_{\mathbf{r}'\sigma'} \right) \\
&\quad - \sum_{\mathbf{r}, \mathbf{r}', \sigma, \sigma'} V_{\mathbf{r}\mathbf{r}'}^{\text{ic}} \left( f_{\mathbf{r}\mathbf{r}'\sigma\sigma'} \bar{f}_{\mathbf{r}\mathbf{r}'\sigma\sigma'}^* - \frac{1}{2} \bar{f}_{\mathbf{r}\mathbf{r}'\sigma\sigma'}^* \bar{f}_{\mathbf{r}\mathbf{r}'\sigma\sigma'} \right) \\
&\quad + \frac{1}{2} \sum_{\mathbf{r}, \mathbf{r}', \sigma, \sigma'} V_{\mathbf{r}\mathbf{r}'}^{\text{ic}} \left( \Delta_{\mathbf{r}\mathbf{r}'\sigma\sigma'} \bar{\Delta}_{\mathbf{r}\mathbf{r}'\sigma\sigma'}^* + \Delta_{\mathbf{r}\mathbf{r}'\sigma\sigma'}^\dagger \bar{\Delta}_{\mathbf{r}\mathbf{r}'\sigma\sigma'} - \bar{\Delta}_{\mathbf{r}\mathbf{r}'\sigma\sigma'} \bar{\Delta}_{\mathbf{r}\mathbf{r}'\sigma\sigma'}^* \right) \quad (\text{A.1})
\end{aligned}$$

390 where the operators are defined as  $n_{\mathbf{r}\sigma} \equiv c_{\mathbf{r}\sigma}^\dagger c_{\mathbf{r}\sigma}$ ,  $f_{\mathbf{r}\mathbf{r}'\sigma\sigma'} \equiv c_{\mathbf{r}\sigma}^\dagger c_{\mathbf{r}'\sigma'}$  and  $\Delta_{\mathbf{r}\mathbf{r}'\sigma\sigma'} \equiv c_{\mathbf{r}\sigma} c_{\mathbf{r}'\sigma'}$ . Note  
391 that the applicability of Wick's theorem is not exact in this case, as we are considering a model  
392 which already includes on-site interactions, but must be considered as an *ad hoc* Ansatz. In  
393 other words, at a fundamental level, we are not assuming that the ground state of the system is  
394 a Slater determinant. We are rather resting on a variational principle for the self-energy [120]  
395 on which CDMFT is formally based.

396 The sum over sites  $\mathbf{r}, \mathbf{r}'$  is taken over the whole lattice. But the average  $\bar{n}_{\mathbf{r}\sigma}$  will be assumed  
397 to have the periodicity of the cluster, i.e.,  $\bar{n}_{\mathbf{r}+\mathbf{R}\sigma} = \bar{n}_{\mathbf{r}\sigma}$  where  $\mathbf{R}$  belongs to the super-lattice. In  
398 addition, the two-site averages  $\bar{f}_{\mathbf{r}\mathbf{r}'\sigma\sigma'}$  and  $\bar{\Delta}_{\mathbf{r}\mathbf{r}'\sigma\sigma'}$  are assumed to depend only on the relative  
399 position  $\mathbf{r} - \mathbf{r}'$ . The mean-field inter-cluster interaction (A.1) is then a one-body contribution  
400 to the Hamiltonian with the periodicity of the super-lattice, and contains both intra-cluster  
401 and inter-cluster terms, whereas the purely intra-cluster part  $V_{\mathbf{r}\mathbf{r}'}^{\text{c}}$  retains its fully correlated  
402 character.

403 For a four-site cluster, we have a total of eight bonds between neighboring clusters, along  
404 the  $x$  and  $y$  directions, with two spin combinations ( $\sigma, \sigma'$ ) per bond, where we consider spin-  
405 parallel combinations for the Fock terms (in the absence of spin-dependent hopping) and spin-  
406 antiparallel combinations for the anomalous terms. In practice, we only consider physically  
407 relevant combinations of operators defined on different sites/bonds for our analysis (such as  
408 those compatible with a  $d$ -wave or an extended  $s$ -wave order). As an illustration of this, let  
409 us consider the pairing fields  $\Delta$  defined on all of these bonds, which we denote by the labels  
410  $i = 1 - 16$  (including different bond and spin combinations).

411 The mean-field Hamiltonian can be written as

$$\frac{V}{2} \sum_{i,j} (\bar{\Delta}_i^* M_{ij} \Delta_j + \Delta_i^\dagger M_{ij} \bar{\Delta}_j - \bar{\Delta}_i^* M_{ij} \bar{\Delta}_j) \quad (\text{A.2})$$

412 where  $i, j = (\mathbf{r}, \mathbf{r}', \sigma, \sigma')$  and the matrix  $M_{ij}$  describes the combinations of the pairing fields  
413 defined on different bonds which appear in the Hartree-Fock decomposition of the intercluster  
414 interactions. The matrix  $M$  turns out to be an identity matrix for the Fock and pairing fields  $f$   
415 and  $\Delta$  respectively, but the corresponding matrix for the Hartree fields  $n$  is off-diagonal.

416 Defining the eigen-combinations of the pairing fields by

$$E_\alpha = U_{\alpha i} \Delta_i \quad (\text{A.3})$$

417 and the eigenvalues of the matrix  $M$  by  $\lambda_\alpha$ , such that

$$M_{ij} = \sum_{\alpha, \beta} U_{\alpha i}^* \lambda_\alpha \delta_{\alpha\beta} U_{\beta j}$$

418 we can rewrite Eq. (A.2), above, as

$$\frac{V}{2} \sum_{\alpha} \lambda_{\alpha} (\bar{E}_{\alpha}^* E_{\alpha} + E_{\alpha}^{\dagger} \bar{E}_{\alpha} - \bar{E}_{\alpha}^* \bar{E}_{\alpha}) \quad (\text{A.4})$$

419 The mean-field values  $\bar{E}_\alpha$  of the relevant eigen-combinations  $E_\alpha$  of the pairing operators de-  
420 fined on different nearest-neighbor bonds are obtained self-consistently within the CDMFT  
421 loop, and likewise for the other mean fields that are the appropriate eigen-combinations of  
422  $\bar{n}_{r\sigma}$  and  $\bar{f}_{rr'\sigma\sigma'}$ .

## 423 References

- 424 [1] H. C. Kao, D. Li and B. Rosenstein, *Unified intermediate coupling description of*  
425 *pseudogap and strange metal phases of cuprates*, Phys. Rev. B **107**, 054508 (2023),  
426 doi:[10.1103/PhysRevB.107.054508](https://doi.org/10.1103/PhysRevB.107.054508).
- 427 [2] T. Li, *A short review of the recent progresses in the study of the cuprate superconductivity\**,  
428 Chinese Physics B **30**(10), 100508 (2021), doi:[10.1088/1674-1056/abfa04](https://doi.org/10.1088/1674-1056/abfa04).
- 429 [3] M. Qin, T. Schäfer, S. Andergassen, P. Corboz and E. Gull, *The Hubbard Model: A Com-*  
430 *putational Perspective*, Annual Review of Condensed Matter Physics **13**(1), 275 (2022),  
431 doi:[10.1146/annurev-conmatphys-090921-033948](https://doi.org/10.1146/annurev-conmatphys-090921-033948).
- 432 [4] H. Tasaki, *The Hubbard model - an introduction and selected rigorous results*,  
433 Journal of Physics: Condensed Matter **10**(20), 4353 (1998), doi:[10.1088/0953-](https://doi.org/10.1088/0953-8984/10/20/004)  
434 [8984/10/20/004](https://doi.org/10.1088/0953-8984/10/20/004).
- 435 [5] D. P. Arovas, E. Berg, S. A. Kivelson and S. Raghu, *The hubbard model*, Annual Review  
436 of Condensed Matter Physics **13**(1), 239 (2022), doi:[10.1146/annurev-conmatphys-](https://doi.org/10.1146/annurev-conmatphys-031620-102024)  
437 [031620-102024](https://doi.org/10.1146/annurev-conmatphys-031620-102024).
- 438 [6] Y. A. Izyumov, *Hubbard model of strong correlations*, Physics-Uspekhi **38**(4), 385 (1995),  
439 doi:[10.1070/PU1995v038n04ABEH000081](https://doi.org/10.1070/PU1995v038n04ABEH000081).
- 440 [7] N. P. Armitage, P. Fournier and R. L. Greene, *Progress and perspectives*  
441 *on electron-doped cuprates*, Reviews of Modern Physics **82**(3), 2421 (2010),  
442 doi:[10.1103/RevModPhys.82.2421](https://doi.org/10.1103/RevModPhys.82.2421).
- 443 [8] M. Atikur Rahman, *A Review on Cuprate Based Superconducting Materials Including*  
444 *Characteristics and Applications*, American Journal of Physics and Applications **3**(2), 39  
445 (2015), doi:[10.11648/j.ajpa.20150302.15](https://doi.org/10.11648/j.ajpa.20150302.15).
- 446 [9] C. Chu, L. Deng and B. Lv, *Hole-doped cuprate high temperature supercon-*  
447 *ductors*, Physica C: Superconductivity and its Applications **514**, 290 (2015),  
448 doi:[10.1016/j.physc.2015.02.047](https://doi.org/10.1016/j.physc.2015.02.047).
- 449 [10] E. Fradkin, S. A. Kivelson and J. M. Tranquada, *Colloquium : Theory of intertwined*  
450 *orders in high temperature superconductors*, Reviews of Modern Physics **87**(2), 457  
451 (2015), doi:[10.1103/RevModPhys.87.457](https://doi.org/10.1103/RevModPhys.87.457).
- 452 [11] E. G. Maksimov, *High-temperature superconductivity: the current state*, Physics-Uspekhi  
453 **43**(10), 965 (2000), doi:[10.1070/PU2000v043n10ABEH000770](https://doi.org/10.1070/PU2000v043n10ABEH000770).
- 454 [12] M. R. Norman and C. Pépin, *The electronic nature of high temperature cuprate super-*  
455 *conductors*, Reports on Progress in Physics **66**(10), 1547 (2003), doi:[10.1088/0034-](https://doi.org/10.1088/0034-4885/66/10/R01)  
456 [4885/66/10/R01](https://doi.org/10.1088/0034-4885/66/10/R01).
- 457 [13] J. Orenstein and A. J. Millis, *Advances in the Physics of High-Temperature Superconduc-*  
458 *tivity*, Science **288**(5465), 468 (2000), doi:[10.1126/science.288.5465.468](https://doi.org/10.1126/science.288.5465.468).

- 459 [14] J. Ruvalds, *Theoretical prospects for high-temperature superconductors*, Superconductor  
460 Science and Technology **9**(11), 905 (1996), doi:[10.1088/0953-2048/9/11/001](https://doi.org/10.1088/0953-2048/9/11/001).
- 461 [15] K. M. Shen and J. S. Davis, *Cuprate high- $T_c$  superconductors*, Materials Today **11**(9), 14  
462 (2008), doi:[10.1016/S1369-7021\(08\)70175-5](https://doi.org/10.1016/S1369-7021(08)70175-5).
- 463 [16] C. M. Varma, *Colloquium : Linear in temperature resistivity and associated mysteries  
464 including high temperature superconductivity*, Reviews of Modern Physics **92**(3), 031001  
465 (2020), doi:[10.1103/RevModPhys.92.031001](https://doi.org/10.1103/RevModPhys.92.031001).
- 466 [17] M. Aichhorn, E. Arrigoni, Z. B. Huang and W. Hanke, *Superconducting Gap in the Hub-  
467 bard Model and the Two-Gap Energy Scales of High-  $T_c$  Cuprate Superconductors*, Physical  
468 Review Letters **99**(25), 257002 (2007), doi:[10.1103/PhysRevLett.99.257002](https://doi.org/10.1103/PhysRevLett.99.257002).
- 469 [18] N. Bulut, D. Scalapino and S. White, *Quasiparticle dispersion in the cuprate superconduc-  
470 tors and the two-dimensional Hubbard model*, Physical Review B **50**(10), 7215 (1994),  
471 doi:[10.1103/PhysRevB.50.7215](https://doi.org/10.1103/PhysRevB.50.7215).
- 472 [19] S. Wermbter and L. Tewordt, *Self-consistent calculation of physical properties for 2D Hub-  
473 bard model and comparison with cuprate superconductors*, Physica C: Superconductivity  
474 **211**(1-2), 132 (1993), doi:[10.1016/0921-4534\(93\)90736-A](https://doi.org/10.1016/0921-4534(93)90736-A).
- 475 [20] M. E. Simón, A. A. Aligia and E. R. Gagliano, *Optical properties of an effective  
476 one-band Hubbard model for the cuprates*, Physical Review B **56**(9), 5637 (1997),  
477 doi:[10.1103/PhysRevB.56.5637](https://doi.org/10.1103/PhysRevB.56.5637).
- 478 [21] F. Simkovic, R. Rossi, A. Georges and M. Ferrero, *Origin and fate of the pseudogap in the  
479 doped Hubbard model*, arXiv:2209.09237 (2022), doi:[10.48550/arXiv.2209.09237](https://doi.org/10.48550/arXiv.2209.09237).
- 480 [22] K. Sheshadri, D. Malterre, A. Fujimori and A. Chainani, *Connecting the one-band and  
481 three-band Hubbard models of cuprates via spectroscopy and scattering experiments*, Phys-  
482 ical Review B **107**(8), 085125 (2023), doi:[10.1103/PhysRevB.107.085125](https://doi.org/10.1103/PhysRevB.107.085125).
- 483 [23] A. Macridin, M. Jarrell, T. Maier and G. A. Sawatzky, *Physics of cuprates with the two-  
484 band Hubbard model: The validity of the one-band Hubbard model*, Physical Review B  
485 **71**(13), 134527 (2005), doi:[10.1103/PhysRevB.71.134527](https://doi.org/10.1103/PhysRevB.71.134527).
- 486 [24] K. Kuroki, R. Arita and H. Aoki, *Link between the spin fluctuation and Fermi surface  
487 in high-  $T_c$  cuprates: A consistent description within the single-band Hubbard model*,  
488 Physical Review B **60**(13), 9850 (1999), doi:[10.1103/PhysRevB.60.9850](https://doi.org/10.1103/PhysRevB.60.9850).
- 489 [25] J. Mußhoff, A. Kiani and E. Pavarini, *Magnetic response trends in cuprates  
490 and the  $t-t'$  Hubbard model*, Physical Review B **103**(7), 075136 (2021),  
491 doi:[10.1103/PhysRevB.103.075136](https://doi.org/10.1103/PhysRevB.103.075136).
- 492 [26] M. Aichhorn, H. G. Evertz, W. von der Linden and M. Potthoff, *Charge ordering in ex-  
493 tended Hubbard models: Variational cluster approach*, Physical Review B **70**(23), 235107  
494 (2004), doi:[10.1103/PhysRevB.70.235107](https://doi.org/10.1103/PhysRevB.70.235107).
- 495 [27] T. Ayral, S. Biermann and P. Werner, *Screening and nonlocal correlations in the extended  
496 Hubbard model from self-consistent combined  $G W$  and dynamical mean field theory*, Phys-  
497 ical Review B **87**(12), 125149 (2013), doi:[10.1103/PhysRevB.87.125149](https://doi.org/10.1103/PhysRevB.87.125149).
- 498 [28] M. Calandra, J. Merino and R. H. McKenzie, *Metal-insulator transition and charge or-  
499 dering in the extended Hubbard model at one-quarter filling*, Physical Review B **66**(19),  
500 195102 (2002), doi:[10.1103/PhysRevB.66.195102](https://doi.org/10.1103/PhysRevB.66.195102).

- 501 [29] J. Callaway, D. P. Chen, D. G. Kanhere and Q. Li, *Small-cluster calculations for*  
502 *the simple and extended Hubbard models*, Physical Review B **42**(1), 465 (1990),  
503 doi:[10.1103/PhysRevB.42.465](https://doi.org/10.1103/PhysRevB.42.465).
- 504 [30] I. M. Carvalho, H. Bragança, W. H. Brito and M. C. O. Aguiar, *Formation of spin and*  
505 *charge ordering in the extended Hubbard model during a finite-time quantum quench*,  
506 Physical Review B **106**(19), 195405 (2022), doi:[10.1103/PhysRevB.106.195405](https://doi.org/10.1103/PhysRevB.106.195405).
- 507 [31] B. Chattopadhyay and D. M. Gaitonde, *Phase diagram of the half-filled extended*  
508 *Hubbard model in two dimensions*, Physical Review B **55**(23), 15364 (1997),  
509 doi:[10.1103/PhysRevB.55.15364](https://doi.org/10.1103/PhysRevB.55.15364).
- 510 [32] W.-C. Chen, Y. Wang and C.-C. Chen, *Superconducting phases of the*  
511 *square-lattice extended hubbard model*, Phys. Rev. B **108**, 064514 (2023),  
512 doi:[10.1103/PhysRevB.108.064514](https://doi.org/10.1103/PhysRevB.108.064514).
- 513 [33] S. N. Coppersmith, *Superconducting states of an extended Hubbard model*, Physical  
514 Review B **42**(4), 2259 (1990), doi:[10.1103/PhysRevB.42.2259](https://doi.org/10.1103/PhysRevB.42.2259).
- 515 [34] B. Davoudi and A.-M. S. Tremblay, *Nearest-neighbor repulsion and competing charge and*  
516 *spin order in the extended Hubbard model*, Physical Review B **74**(3), 035113 (2006),  
517 doi:[10.1103/PhysRevB.74.035113](https://doi.org/10.1103/PhysRevB.74.035113).
- 518 [35] B. Davoudi and A.-M. S. Tremblay, *Non-perturbative treatment of charge and*  
519 *spin fluctuations in the two-dimensional extended Hubbard model: Extended two-*  
520 *particle self-consistent approach*, Physical Review B **76**(8), 085115 (2007),  
521 doi:[10.1103/PhysRevB.76.085115](https://doi.org/10.1103/PhysRevB.76.085115).
- 522 [36] R. Fresard and V. H. Dao, *Charge instabilities of the extended attractive Hubbard*  
523 *Model on the cubic lattice*, Modern Physics Letters B **34**(19n20), 2040050 (2020),  
524 doi:[10.1142/S0217984920400503](https://doi.org/10.1142/S0217984920400503).
- 525 [37] V. F. Gilmutdinov, M. A. Timirgazin and A. K. Arzhnikov, *Interplay of magnetism and*  
526 *superconductivity in 2D extended Hubbard model*, Journal of Magnetism and Magnetic  
527 Materials **560**, 169605 (2022), doi:[10.1016/j.jmmm.2022.169605](https://doi.org/10.1016/j.jmmm.2022.169605).
- 528 [38] S. R. Hassan and L. de' Medici, *Slave spins away from half filling: Cluster mean-field*  
529 *theory of the Hubbard and extended Hubbard models*, Physical Review B **81**(3), 035106  
530 (2010), doi:[10.1103/PhysRevB.81.035106](https://doi.org/10.1103/PhysRevB.81.035106).
- 531 [39] W.-M. Huang, C.-Y. Lai, C. Shi and S.-W. Tsai, *Unconventional superconducting phases*  
532 *for the two-dimensional extended Hubbard model on a square lattice*, Physical Review B  
533 **88**(5), 054504 (2013), doi:[10.1103/PhysRevB.88.054504](https://doi.org/10.1103/PhysRevB.88.054504).
- 534 [40] J. Jędrzejewski, *Phase diagrams of extended Hubbard models in the atomic limit*, Physica  
535 A: Statistical Mechanics and its Applications **205**(4), 702 (1994), doi:[10.1016/0378-](https://doi.org/10.1016/0378-4371(94)90231-3)  
536 [4371\(94\)90231-3](https://doi.org/10.1016/0378-4371(94)90231-3).
- 537 [41] M. Y. Kagan, D. V. Efremov, M. S. Marienko and V. V. Val'kov, *Triplet p-wave superconduct-*  
538 *ivity in the low-density extended hubbard model with Coulomb repulsion*, JETP Letters  
539 **93**(12), 725 (2011), doi:[10.1134/S0021364011120083](https://doi.org/10.1134/S0021364011120083).
- 540 [42] K. J. Kapcia, S. Robaszkiewicz, M. Capone and A. Amaricci, *Doping-driven metal-*  
541 *insulator transitions and charge orderings in the extended Hubbard model*, Physical Re-  
542 view B **95**(12), 125112 (2017), doi:[10.1103/PhysRevB.95.125112](https://doi.org/10.1103/PhysRevB.95.125112).



- 543 [43] K. Kapcia and S. Robaszkiewicz, *The effects of the next-nearest-neighbour density–density*  
544 *interaction in the atomic limit of the extended Hubbard model*, Journal of Physics: Con-  
545 densed Matter **23**(24), 249802 (2011), doi:[10.1088/0953-8984/23/24/249802](https://doi.org/10.1088/0953-8984/23/24/249802).
- 546 [44] E. Linnér, C. Dutreix, S. Biermann and E. A. Stepanov, *Coexistence of s-wave supercon-*  
547 *ductivity and phase separation in the half-filled extended Hubbard model with attractive*  
548 *interactions*, arXiv:2301.10755 (2023), doi:[10.48550/arXiv.2301.10755](https://doi.org/10.48550/arXiv.2301.10755).
- 549 [45] E. Linnér, A. I. Lichtenstein, S. Biermann and E. A. Stepanov, *Multichannel fluctuating*  
550 *field approach to competing instabilities in interacting electronic systems*, Phys. Rev. B  
551 **108**, 035143 (2023), doi:[10.1103/PhysRevB.108.035143](https://doi.org/10.1103/PhysRevB.108.035143).
- 552 [46] P. B. Littlewood, *Collective modes and superconductivity in an extended Hubbard*  
553 *model for copper oxide superconductors*, Physical Review B **42**(16), 10075 (1990),  
554 doi:[10.1103/PhysRevB.42.10075](https://doi.org/10.1103/PhysRevB.42.10075).
- 555 [47] P. B. Littlewood, C. M. Varma and E. Abrahams, *Pairing instabilities of the extended*  
556 *Hubbard model for Cu-O – based superconductors*, Physical Review Letters **63**(23), 2602  
557 (1989), doi:[10.1103/PhysRevLett.63.2602](https://doi.org/10.1103/PhysRevLett.63.2602).
- 558 [48] J. Merino, *Nonlocal Coulomb Correlations in Metals Close to a Charge Or-*  
559 *der Insulator Transition*, Physical Review Letters **99**(3), 036404 (2007),  
560 doi:[10.1103/PhysRevLett.99.036404](https://doi.org/10.1103/PhysRevLett.99.036404).
- 561 [49] J. Merino and R. H. McKenzie, *Superconductivity Mediated by Charge Fluctuations*  
562 *in Layered Molecular Crystals*, Physical Review Letters **87**(23), 237002 (2001),  
563 doi:[10.1103/PhysRevLett.87.237002](https://doi.org/10.1103/PhysRevLett.87.237002).
- 564 [50] R. Micnas, J. Ranninger and S. Robaszkiewicz, *An extended Hubbard model with inter-*  
565 *site attraction in two dimensions and high- $T_c$  superconductivity*, Journal of Physics C:  
566 Solid State Physics **21**(6), L145 (1988), doi:[10.1088/0022-3719/21/6/009](https://doi.org/10.1088/0022-3719/21/6/009).
- 567 [51] R. Micnas, J. Ranninger, S. Robaszkiewicz and S. Tabor, *Superconductivity in a narrow-*  
568 *band system with intersite electron pairing in two dimensions: A mean-field study*, Physical  
569 Review B **37**(16), 9410 (1988), doi:[10.1103/PhysRevB.37.9410](https://doi.org/10.1103/PhysRevB.37.9410).
- 570 [52] R. Micnas, J. Ranninger and S. Robaszkiewicz, *Superconductivity in a narrow-*  
571 *band system with intersite electron pairing in two dimensions. II. Effects of nearest-*  
572 *neighbor exchange and correlated hopping*, Physical Review B **39**(16), 11653 (1989),  
573 doi:[10.1103/PhysRevB.39.11653](https://doi.org/10.1103/PhysRevB.39.11653).
- 574 [53] R. Micnas and B. Tobijaszewska, *Superfluid properties of the extended Hubbard model*  
575 *with intersite electron pairing*, Journal of Physics: Condensed Matter **14**(41), 9631  
576 (2002), doi:[10.1088/0953-8984/14/41/319](https://doi.org/10.1088/0953-8984/14/41/319).
- 577 [54] M. Murakami, *Possible Ordered States in the 2D Extended Hubbard Model*, Journal of the  
578 Physical Society of Japan **69**(4), 1113 (2000), doi:[10.1143/JPSJ.69.1113](https://doi.org/10.1143/JPSJ.69.1113).
- 579 [55] Y. Ohta, K. Tsutsui, W. Koshibae and S. Maekawa, *Exact-diagonalization study of the Hub-*  
580 *bard model with nearest-neighbor repulsion*, Physical Review B **50**(18), 13594 (1994),  
581 doi:[10.1103/PhysRevB.50.13594](https://doi.org/10.1103/PhysRevB.50.13594).
- 582 [56] S. Onari, R. Arita, K. Kuroki and H. Aoki, *Phase diagram of the two-dimensional ex-*  
583 *tended Hubbard model: Phase transitions between different pairing symmetries when*  
584 *charge and spin fluctuations coexist*, Physical Review B **70**(9), 094523 (2004),  
585 doi:[10.1103/PhysRevB.70.094523](https://doi.org/10.1103/PhysRevB.70.094523).

- 586 [57] C. Peng, Y. Wang, J. Wen, Y. S. Lee, T. P. Devereaux and H.-C. Jiang, *Enhanced super-*  
587 *conductivity by near-neighbor attraction in the doped extended Hubbard model*, Physical  
588 Review B **107**(20), L201102, doi:[10.1103/PhysRevB.107.L201102](https://doi.org/10.1103/PhysRevB.107.L201102).
- 589 [58] L. Philoxene, V. H. Dao and R. Frésard, *Spin and charge modulations of a*  
590 *half-filled extended Hubbard model*, Physical Review B **106**(23), 235131 (2022),  
591 doi:[10.1103/PhysRevB.106.235131](https://doi.org/10.1103/PhysRevB.106.235131).
- 592 [59] R. Pietig, R. Bulla and S. Blawid, *Reentrant Charge Order Transition in*  
593 *the Extended Hubbard Model*, Physical Review Letters **82**(20), 4046 (1999),  
594 doi:[10.1103/PhysRevLett.82.4046](https://doi.org/10.1103/PhysRevLett.82.4046).
- 595 [60] N. M. Plakida and V. S. Oudovenko, *On the theory of superconductivity in the extended*  
596 *Hubbard model: Spin-fluctuation pairing*, The European Physical Journal B **86**(3), 115  
597 (2013), doi:[10.1140/epjb/e2013-31157-6](https://doi.org/10.1140/epjb/e2013-31157-6).
- 598 [61] N. Plonka, C. J. Jia, Y. Wang, B. Moritz and T. P. Devereaux, *Fidelity study of super-*  
599 *conductivity in extended Hubbard models*, Physical Review B **92**(2), 024503 (2015),  
600 doi:[10.1103/PhysRevB.92.024503](https://doi.org/10.1103/PhysRevB.92.024503).
- 601 [62] P. Pudleiner, A. Kauch, K. Held and G. Li, *Competition between antiferromagnetic and*  
602 *charge density wave fluctuations in the extended Hubbard model*, Physical Review B  
603 **100**(7), 075108 (2019), doi:[10.1103/PhysRevB.100.075108](https://doi.org/10.1103/PhysRevB.100.075108).
- 604 [63] S. Raghu, E. Berg, A. V. Chubukov and S. A. Kivelson, *Effects of longer-range interac-*  
605 *tions on unconventional superconductivity*, Physical Review B **85**(2), 024516 (2012),  
606 doi:[10.1103/PhysRevB.85.024516](https://doi.org/10.1103/PhysRevB.85.024516).
- 607 [64] M. Roig, A. T. Rømer, P. J. Hirschfeld and B. M. Andersen, *Revisiting superconductivity in*  
608 *the extended one-band Hubbard model: pairing via spin and charge fluctuations*, Physical  
609 Review B **106**(21), 214530 (2022), doi:[10.1103/PhysRevB.106.214530](https://doi.org/10.1103/PhysRevB.106.214530).
- 610 [65] K. Rościszewski and A. M. Oleś, *Charge order in the extended hubbard model*,  
611 Journal of Physics: Condensed Matter **15**(49), 8363 (2003), doi:[10.1088/0953-](https://doi.org/10.1088/0953-8984/15/49/014)  
612 [8984/15/49/014](https://doi.org/10.1088/0953-8984/15/49/014).
- 613 [66] K. Rosciszewski and A. M. Oles, *Pair binding in small clusters described by the ex-*  
614 *tended Hubbard model*, Journal of Physics: Condensed Matter **7**(3), 657 (1995),  
615 doi:[10.1088/0953-8984/7/3/019](https://doi.org/10.1088/0953-8984/7/3/019).
- 616 [67] M. Schüler, E. G. C. P. Van Loon, M. I. Katsnelson and T. O. Wehling, *First-*  
617 *order metal-insulator transitions in the extended Hubbard model due to self-consistent*  
618 *screening of the effective interaction*, Physical Review B **97**(16), 165135 (2018),  
619 doi:[10.1103/PhysRevB.97.165135](https://doi.org/10.1103/PhysRevB.97.165135).
- 620 [68] M. Schüler, E. Van Loon, M. Katsnelson and T. Wehling, *Thermodynamics of the metal-*  
621 *insulator transition in the extended Hubbard model*, SciPost Physics **6**(6), 067 (2019),  
622 doi:[10.21468/SciPostPhys.6.6.067](https://doi.org/10.21468/SciPostPhys.6.6.067).
- 623 [69] A. Sherman, *Two-dimensional extended hubbard model: doping, next-nearest*  
624 *neighbor hopping and phase diagrams*, Physica Scripta **98**(11), 115947 (2023),  
625 doi:[10.1088/1402-4896/ad000b](https://doi.org/10.1088/1402-4896/ad000b).
- 626 [70] S. d. A. Sousa-Júnior, N. C. Costa and R. R. d. Santos, *Phase diagram for*  
627 *the extended Hubbard model on a square lattice*, arXiv:2304.08683 (2023),  
628 doi:[10.48550/arXiv.2304.08683](https://doi.org/10.48550/arXiv.2304.08683).

- 629 [71] W. P. Su, *Phase separation and  $d$ -wave superconductivity in a two-dimensional extended*  
630 *Hubbard model with nearest-neighbor attractive interaction*, Physical Review B **69**(1),  
631 012506 (2004), doi:[10.1103/PhysRevB.69.012506](https://doi.org/10.1103/PhysRevB.69.012506).
- 632 [72] W. P. Su and Y. Chen, *Spin-density wave and superconductivity in an extended two-*  
633 *dimensional Hubbard model with nearest-neighbor attraction*, Physical Review B **64**(17),  
634 172507 (2001), doi:[10.1103/PhysRevB.64.172507](https://doi.org/10.1103/PhysRevB.64.172507).
- 635 [73] Z. Sun and H.-Q. Lin, *Exploring high-temperature superconductivity in the ex-*  
636 *tended hubbard model with antiferromagnetic tendencies*, arXiv:2304.07490 (2023),  
637 doi:[10.48550/arXiv.2304.07490](https://doi.org/10.48550/arXiv.2304.07490).
- 638 [74] A. Sushcheyev and S. Wessel, *Thermodynamics of the metal-insulator transition in the*  
639 *extended Hubbard model from determinantal quantum Monte Carlo*, Physical Review B  
640 **106**(15), 155121 (2022), doi:[10.1103/PhysRevB.106.155121](https://doi.org/10.1103/PhysRevB.106.155121).
- 641 [75] Z. Szabó and Z. Gulácsi, *Superconducting phases of the extended Hubbard*  
642 *model for doped systems*, Czechoslovak Journal of Physics **46**(S2), 609 (1996),  
643 doi:[10.1007/BF02583612](https://doi.org/10.1007/BF02583612).
- 644 [76] H. Terletska, T. Chen and E. Gull, *Charge ordering and correlation effects*  
645 *in the extended Hubbard model*, Physical Review B **95**(11), 115149 (2017),  
646 doi:[10.1103/PhysRevB.95.115149](https://doi.org/10.1103/PhysRevB.95.115149).
- 647 [77] H. Terletska, T. Chen, J. Paki and E. Gull, *Charge ordering and non-local correlations*  
648 *in the doped extended Hubbard model*, Physical Review B **97**(11), 115117 (2018),  
649 doi:[10.1103/PhysRevB.97.115117](https://doi.org/10.1103/PhysRevB.97.115117).
- 650 [78] H. Terletska, S. Isakov, T. Maier and E. Gull, *Dynamical Cluster Approximation Study of*  
651 *Electron Localization in the Extended Hubbard Model*, Physical Review B **104**(8), 085129  
652 (2021), doi:[10.1103/PhysRevB.104.085129](https://doi.org/10.1103/PhysRevB.104.085129).
- 653 [79] N.-H. Tong, S.-Q. Shen and R. Bulla, *Charge ordering and phase separation in the in-*  
654 *finite dimensional extended Hubbard model*, Physical Review B **70**(8), 085118 (2004),  
655 doi:[10.1103/PhysRevB.70.085118](https://doi.org/10.1103/PhysRevB.70.085118).
- 656 [80] P. G. J. van Dongen, *Thermodynamics of the extended Hubbard model in high dimensions*,  
657 Physical Review Letters **67**(6), 757 (1991), doi:[10.1103/PhysRevLett.67.757](https://doi.org/10.1103/PhysRevLett.67.757).
- 658 [81] E. G. C. P. van Loon and M. I. Katsnelson, *The extended Hubbard model with at-*  
659 *tractive interactions*, Journal of Physics: Conference Series **1136**, 012006 (2018),  
660 doi:[10.1088/1742-6596/1136/1/012006](https://doi.org/10.1088/1742-6596/1136/1/012006).
- 661 [82] M. Vandelli, V. Harkov, E. A. Stepanov, J. Gukelberger, E. Kozik, A. Rubio  
662 and A. I. Lichtenstein, *Dual boson diagrammatic Monte Carlo approach applied*  
663 *to the extended Hubbard model*, Physical Review B **102**(19), 195109 (2020),  
664 doi:[10.1103/PhysRevB.102.195109](https://doi.org/10.1103/PhysRevB.102.195109).
- 665 [83] M. Vojta, A. Hübsch and R. M. Noack, *Phase diagram of the quarter-filled extended*  
666 *Hubbard model on a two-leg ladder*, Physical Review B **63**(4), 045105 (2001),  
667 doi:[10.1103/PhysRevB.63.045105](https://doi.org/10.1103/PhysRevB.63.045105).
- 668 [84] H.-X. Wang, Y.-M. Wu, Y.-F. Jiang and H. Yao, *Spectral properties of 1D extended Hubbard*  
669 *model from bosonization and time-dependent variational principle: applications to 1D*  
670 *cuprate*, arXiv:2211.02031 (2022), doi:[10.48550/arXiv.2211.02031](https://doi.org/10.48550/arXiv.2211.02031).

- 671 [85] S. Wolf, T. L. Schmidt and S. Rachel, *Unconventional superconductivity in the extended*  
672 *Hubbard model: Weak-coupling renormalization group*, Physical Review B **98**(17),  
673 174515 (2018), doi:[10.1103/PhysRevB.98.174515](https://doi.org/10.1103/PhysRevB.98.174515).
- 674 [86] X.-Z. Yan, *Theory of the extended Hubbard model at half filling*, Physical Review B **48**(10),  
675 7140 (1993), doi:[10.1103/PhysRevB.48.7140](https://doi.org/10.1103/PhysRevB.48.7140).
- 676 [87] M. Yao, D. Wang and Q.-H. Wang, *Determinant quantum Monte Carlo for the half-filled*  
677 *Hubbard model with nonlocal density-density interactions*, Physical Review B **106**(19),  
678 195121 (2022), doi:[10.1103/PhysRevB.106.195121](https://doi.org/10.1103/PhysRevB.106.195121).
- 679 [88] K. Yoshimi, T. Kato and H. Maebashi, *Enhanced Spin Susceptibility toward the Charge-*  
680 *Ordering Transition in a Two-Dimensional Extended Hubbard Model*, Journal of the Phys-  
681 ical Society of Japan **78**(10), 104002 (2009), doi:[10.1143/JPSJ.78.104002](https://doi.org/10.1143/JPSJ.78.104002).
- 682 [89] Y. Zhang and J. Callaway, *Extended Hubbard model in two dimensions*, Physical Review  
683 B **39**(13), 9397 (1989), doi:[10.1103/PhysRevB.39.9397](https://doi.org/10.1103/PhysRevB.39.9397).
- 684 [90] Z. Zhou, W. Ye, H.-G. Luo, J. Zhao and J. Chang, *Robust superconducting correlation*  
685 *against intersite interactions in the extended two-leg hubbard ladder*, Phys. Rev. B **108**,  
686 195136 (2023), doi:[10.1103/PhysRevB.108.195136](https://doi.org/10.1103/PhysRevB.108.195136).
- 687 [91] Z. Chen, Y. Wang, S. N. Rebec, T. Jia, M. Hashimoto, D. Lu, B. Moritz, R. G. Moore,  
688 T. P. Devereaux and Z.-X. Shen, *Anomalously strong near-neighbor attraction in doped*  
689 *1D cuprate chains*, Science **373**(6560), 1235 (2021), doi:[10.1126/science.abf5174](https://doi.org/10.1126/science.abf5174).
- 690 [92] M. Jiang, U. R. Hähner, T. C. Schulthess and T. A. Maier, *d-wave superconductivity in*  
691 *the presence of nearest-neighbor Coulomb repulsion*, Physical Review B **97**(18), 184507  
692 (2018), doi:[10.1103/PhysRevB.97.184507](https://doi.org/10.1103/PhysRevB.97.184507).
- 693 [93] H. Hu, L. Chen and Q. Si, *Extended Dynamical Mean Field Theory for Correlated Electron*  
694 *Models*, arXiv:2210.14197 (2022), doi:[10.48550/arXiv.2210.14197](https://doi.org/10.48550/arXiv.2210.14197).
- 695 [94] L. Huang, T. Ayal, S. Biermann and P. Werner, *Extended dynamical mean-field study*  
696 *of the Hubbard model with long-range interactions*, Physical Review B **90**(19), 195114  
697 (2014), doi:[10.1103/PhysRevB.90.195114](https://doi.org/10.1103/PhysRevB.90.195114).
- 698 [95] R. Chitra and G. Kotliar, *Effect of Long Range Coulomb Interactions on the Mott Transition*,  
699 Physical Review Letters **84**(16), 3678 (2000), doi:[10.1103/PhysRevLett.84.3678](https://doi.org/10.1103/PhysRevLett.84.3678).
- 700 [96] T. Ayal, P. Werner and S. Biermann, *Spectral Properties of Correlated Materi-*  
701 *als: Local Vertex and Nonlocal Two-Particle Correlations from Combined G W and*  
702 *Dynamical Mean Field Theory*, Physical Review Letters **109**(22), 226401 (2012),  
703 doi:[10.1103/PhysRevLett.109.226401](https://doi.org/10.1103/PhysRevLett.109.226401).
- 704 [97] P. Sun and G. Kotliar, *Extended dynamical mean-field theory and GW method*, Physical  
705 Review B **66**(8), 085120 (2002), doi:[10.1103/PhysRevB.66.085120](https://doi.org/10.1103/PhysRevB.66.085120).
- 706 [98] P. Sun and G. Kotliar, *Many-Body Approximation Scheme beyond GW*, Physical Review  
707 Letters **92**(19), 196402 (2004), doi:[10.1103/PhysRevLett.92.196402](https://doi.org/10.1103/PhysRevLett.92.196402).
- 708 [99] E. G. C. P. van Loon, A. I. Lichtenstein, M. I. Katsnelson, O. Parcollet and H. Hafer-  
709 mann, *Beyond extended dynamical mean-field theory: Dual boson approach to the*  
710 *two-dimensional extended Hubbard model*, Physical Review B **90**(23), 235135 (2014),  
711 doi:[10.1103/PhysRevB.90.235135](https://doi.org/10.1103/PhysRevB.90.235135).

- 712 [100] G. Kotliar, S. Y. Savrasov, G. Pálsson and G. Biroli, *Cellular Dynamical Mean Field Ap-*  
713 *proach to Strongly Correlated Systems*, Physical Review Letters **87**(18), 186401 (2001),  
714 doi:[10.1103/PhysRevLett.87.186401](https://doi.org/10.1103/PhysRevLett.87.186401).
- 715 [101] N.-H. Tong, *Extended variational cluster approximation for correlated systems*, Physical  
716 Review B **72**(11), 115104 (2005), doi:[10.1103/PhysRevB.72.115104](https://doi.org/10.1103/PhysRevB.72.115104).
- 717 [102] A. I. Lichtenstein and M. I. Katsnelson, *Antiferromagnetism and d-wave superconductivity*  
718 *in cuprates: A cluster dynamical mean-field theory*, Phys. Rev. B **62**(14), R9283 (2000),  
719 doi:[10.1103/PhysRevB.62.R9283](https://doi.org/10.1103/PhysRevB.62.R9283).
- 720 [103] T. Maier, M. Jarrell, T. Pruschke and M. H. Hettler, *Quantum cluster theories*, Rev. Mod.  
721 Phys. **77**(3), 1027 (2005), doi:[10.1103/RevModPhys.77.1027](https://doi.org/10.1103/RevModPhys.77.1027).
- 722 [104] G. D. Adebajo, J. P. Hague and P. E. Kornilovitch, *Ubiquity of light small pairs in*  
723 *Hubbard models with long range hoppings and interactions*, arXiv:2211.06498 (2022),  
724 doi:[10.48550/arXiv.2211.06498](https://doi.org/10.48550/arXiv.2211.06498).
- 725 [105] D. Sénéchal, *Cluster Dynamical Mean Field Theory*, In A. Avella and F. Mancini, eds.,  
726 *Strongly Correlated Systems*, vol. 171, pp. 341–371. Springer Berlin Heidelberg, Berlin,  
727 Heidelberg, ISBN 978-3-642-21830-9 978-3-642-21831-6, doi:[10.1007/978-3-642-](https://doi.org/10.1007/978-3-642-21831-6_11)  
728 [21831-6\\_11](https://doi.org/10.1007/978-3-642-21831-6_11), Series Title: Springer Series in Solid-State Sciences (2012).
- 729 [106] D. Sénéchal, *Cluster Perturbation Theory*, In A. Avella and F. Mancini, eds., *Strongly Cor-*  
730 *related Systems*, vol. 171, pp. 237–270. Springer Berlin Heidelberg, Berlin, Heidelberg,  
731 ISBN 978-3-642-21830-9 978-3-642-21831-6, doi:[10.1007/978-3-642-21831-6\\_8](https://doi.org/10.1007/978-3-642-21831-6_8), Se-  
732 ries Title: Springer Series in Solid-State Sciences (2012).
- 733 [107] D. Sénéchal, *The Variational Cluster Approximation for Hubbard Models: Practical Im-*  
734 *plementation*, In *2008 22nd International Symposium on High Performance Computing*  
735 *Systems and Applications*, pp. 9–15. IEEE, Quebec city, QC, Canada, ISBN 978-0-7695-  
736 3250-9, doi:[10.1109/HPCS.2008.18](https://doi.org/10.1109/HPCS.2008.18), ISSN: 1550-5243 (2008).
- 737 [108] D. Sénéchal, *An introduction to quantum cluster methods*, arXiv:0806.2690 (2008),  
738 doi:[10.48550/arXiv.0806.2690](https://doi.org/10.48550/arXiv.0806.2690).
- 739 [109] C. Slezak, M. Jarrell, T. Maier and J. Deisz, *Multi-scale extensions to quantum cluster*  
740 *methods for strongly correlated electron systems*, Journal of Physics: Condensed Matter  
741 **21**(43), 435604 (2009), doi:[10.1088/0953-8984/21/43/435604](https://doi.org/10.1088/0953-8984/21/43/435604).
- 742 [110] T. N. Dionne, A. Foley, M. Rousseau and D. Senechal, *Pyqcm: An open-*  
743 *source python library for quantum cluster methods*, arXiv:2305.18643 (2023),  
744 doi:[10.48550/arXiv.2305.18643](https://doi.org/10.48550/arXiv.2305.18643).
- 745 [111] A. Georges, G. Kotliar, W. Krauth and M. J. Rozenberg, *Dynamical mean-field theory*  
746 *of strongly correlated fermion systems and the limit of infinite dimensions*, Reviews of  
747 Modern Physics **68**(1), 13 (1996), doi:[10.1103/RevModPhys.68.13](https://doi.org/10.1103/RevModPhys.68.13).
- 748 [112] A. Georges, *Strongly Correlated Electron Materials: Dynamical Mean-Field Theory and*  
749 *Electronic Structure*, In *AIP Conference Proceedings*, vol. 715, pp. 3–74. AIP, Salerno  
750 (Italy), doi:[10.1063/1.1800733](https://doi.org/10.1063/1.1800733), ISSN: 0094243X (2004).
- 751 [113] K. Held, *Electronic structure calculations using dynamical mean field theory*, Advances  
752 in Physics **56**(6), 829 (2007), doi:[10.1080/00018730701619647](https://doi.org/10.1080/00018730701619647).

- 753 [114] D. Vollhardt, *Dynamical Mean-Field Theory of Strongly Correlated Electron Systems*,  
754 In *Proceedings of the International Conference on Strongly Correlated Electron Systems*  
755 (*SCES2019*). Journal of the Physical Society of Japan, Okayama, Japan, ISBN 978-4-  
756 89027-142-9, doi:[10.7566/JPSCP30.011001](https://doi.org/10.7566/JPSCP30.011001) (2020).
- 757 [115] E. Dagotto, J. Riera, Y. C. Chen, A. Moreo, A. Nazarenko, F. Alcaraz and F. Ortolani,  
758 *Superconductivity near phase separation in models of correlated electrons*, Physical Review  
759 B **49**(5), 3548 (1994), doi:[10.1103/PhysRevB.49.3548](https://doi.org/10.1103/PhysRevB.49.3548).
- 760 [116] B. Kyung, D. Sénéchal and A.-M. S. Tremblay, *Pairing dynamics in strongly*  
761 *correlated superconductivity*, Physical Review B **80**(20), 205109 (2009),  
762 doi:[10.1103/PhysRevB.80.205109](https://doi.org/10.1103/PhysRevB.80.205109).
- 763 [117] D. Sénéchal, A. G. R. Day, V. Bouliane and A.-M. S. Tremblay, *Resilience of d-wave su-*  
764 *perconductivity to nearest-neighbor repulsion*, Physical Review B **87**(7), 75123 (2013),  
765 doi:[10.1103/PhysRevB.87.075123](https://doi.org/10.1103/PhysRevB.87.075123).
- 766 [118] N. Kowalski, S. S. Dash, P. Sémon, D. Sénéchal and A.-M. Tremblay, *Oxygen hole content,*  
767 *charge-transfer gap, covalency, and cuprate superconductivity*, PNAS **118**, e2106476118  
768 (2021), doi:[10.1073/pnas.2106476118](https://doi.org/10.1073/pnas.2106476118).
- 769 [119] R. Scholle, P. M. Bonetti, D. Vilardi and W. Metzner, *Comprehensive mean-field analysis*  
770 *of magnetic and charge orders in the two-dimensional hubbard model*, Phys. Rev. B **108**,  
771 035139 (2023), doi:[10.1103/PhysRevB.108.035139](https://doi.org/10.1103/PhysRevB.108.035139).
- 772 [120] M. Potthoff, *Self-energy-functional approach to systems of correlated electrons*, European  
773 Physical Journal B **32**(4), 429 (2003), doi:[10.1140/epjb/e2003-00121-8](https://doi.org/10.1140/epjb/e2003-00121-8).